CCAMLR

Commission for the Conservation of Antarctic Marine Living Resources
Commission pour la conservation de la faune et la flore marines de l'Antarctique
Комиссия по сохранению морских живых ресурсов Антарктики
Comisión para la Conservación de los Recursos Vivos Marinos Antárticos

WG-FSA-2025/25

20 September 2025

Original: English

WG-FSA

Temperature variation associated with interannual variability in abundance of juvenile Patagonian toothfish (Dissostichus eleginoides) at South Georgia

Cavanagh, R.D., T. Jones, S.E. Thorpe, J. Cleeland, T. Earl, J.J. Freer, S.L. Hill , O.T. Hogg, P.R. Hollyman, C.M. Waluda and M.A. Collins

Temperature variation associated with interannual variability in abundance of juvenile Patagonian toothfish (*Dissostichus eleginoides*) at South Georgia

*R. D. Cavanagh[1], *T. Jones[1], S. E. Thorpe[1], J. Cleeland[1], T. Earl[2], J. J. Freer[1], S. L. Hill [1], O. T. Hogg[2], P. R. Hollyman[3], C. M. Waluda[1] and M. A. Collins[1]

*Joint first authors
[1]British Antarctic Survey, NERC, Cambridge, UK
[2]Centre of Environment Fisheries and Aquaculture Science (Cefas), Lowestoft, UK
[3]School of Ocean Sciences, Bangor University, Askew Street, Menai Bridge, LL59 5AB, UK

Abstract

A detailed understanding of the life cycles of fished species in relation to their environment is important for predicting the impacts of environmental change and integrating these considerations into management to ensure long-term sustainability. Here, we present findings from a study exploring the relationship between the abundance of early life stages of Patagonian toothfish (*Dissostichus eleginoides*) and temperature in the waters around the sub-Antarctic island of South Georgia and nearby Shag Rocks (Subarea 48.3). Using counts and size data of Patagonian toothfish collected during demersal trawls performed on the South Georgia and Shag Rocks shelf (1986-2023), we constructed a series of models relating interannual variability in juvenile (< 26 cm and 26-37 cm size-classes) abundance to regional temperatures during spawning, egg-dispersal, larval-dispersal, and post-benthic settlement developmental stages. During those analyses, we considered temperatures at multiple depth-strata, ranging from the surface to the seafloor, informed by the known distribution of Patagonian toothfish during those stages of development. We then evaluated long-term trends in temperature to identify stages that have potentially experienced the largest changes in thermal conditions over the last 30 years. Juvenile Patagonian toothfish showed marked interannual variability overlaid onto an apparent long-term decline in abundance from 1987 to 2023. Interannual variation in abundance of juveniles was highly correlated with sub-surface temperatures during the spawning and egg-dispersal time-windows, with cooler temperatures associated with lower abundance. While

regional sea surface temperatures increased from 1993 to 2023, temperatures below the surface mixed layer during the spawning period appear to have decreased, which may be contributing to the apparent decline in juvenile abundance. This study contributes to the work of WG-FSA in progressing recommendations from the CCAMLR Workshop on Climate Change, particularly in relation to drivers of distribution and inter-annual variability in abundance and recruitment patterns. Our findings underscore the importance of considering factors beyond sea surface temperature changes when assessing the impacts of climate change on fished species, as well as the role of environmental conditions across key developmental windows. Understanding these drivers provides the opportunity for future recruitment assumptions used in management to be based on an understanding of the underlying processes, rather than empirical approaches, ultimately leading to more informed and effective decision-making.

Introduction

Understanding the dynamics and distribution of commercially exploited fish in relation to environmental factors is essential for effective fisheries management. High-latitude fish species are particularly relevant in this context, given their sensitivity to environmental variability and occurrence in ecosystems undergoing accelerated, climate-driven changes (Frainer et al., 2017; Campana et al., 2020). Life stages vary in their sensitivity and exposure to changing environmental conditions, influenced by factors such as physiology (e.g., thermal tolerance), horizontal and vertical distribution (e.g. dispersal ability, ontogenetic migration (Collins et al., 2005)), and trophic position (Freer et al., 2019). This sensitivity can be especially pronounced during early life stages, where environmental conditions can play a critical role in determining survival and recruitment success (Howard et al., 2024). A key driver is temperature, known to influence physiology, development, phenology, recruitment and survival in high-latitude species such as Arctic cod (*Boreogadus saida*) and Walleye pollock (*Theragra chalcogramma*) (Laurel et al., 2018; Huserbråten et al., 2019; IPCC 2019; Ljungström et al., 2021; Levine et al., 2023).

However, early life stages are often less well understood and consequently underrepresented in stock assessment models and fisheries management compared to adult fish (Gross & Hoenig 2025). Gaining a detailed understanding of exploited species throughout their life stages is crucial for more accurately predicting the impacts of environmental change and integrating these considerations into management.

Here we focus on Patagonian toothfish (*Dissostichus eleginoides* Smitt 1898), a commercially fished notothenioid with a circumpolar distribution around islands and continental shelves in the Southern Ocean and South Atlantic, including the sub-Antarctic islands of South Georgia and Shag Rocks which are the focus of this study (**Figure 1**). The Patagonian toothfish population at South Georgia, Shag Rocks, and the northern South Sandwich Islands, is considered a largely self-contained stock with limited connectivity to other populations and lies at the southern limit of the species' distribution (Shaw et al., 2004; Collins et al., 2010; Rogers et al., 2006; Soeffker et al., 2022; Jones et al., 2025). While we note that Arkhipkin et al. (2022) proposed that stocks of *D. eleginoides* on the Patagonian Shelf and at South Georgia are sufficiently distinct to be considered separate species, this has yet to be verified and hence we continue to use *D. eleginoides* for both populations.

South Georgia and Shag Rocks are part of the Scotia Arc, a predominantly submarine ridge that forms the perimeter of the Scotia Sea. The South Georgia and Shag Rocks shelves (average depth ≈ 200 m; Gregory et al., 2017) are separated by a deep canyon (maximum depth of 2000 m) and lie in the Antarctic Circumpolar Current (ACC), to the south of the Polar Front. Shag Rocks, located closer to the Polar Front, typically experiences warmer surface conditions than around South Georgia, as waters around South Georgia are more strongly influenced by cooler subpolar waters given its proximity to the Southern ACC Front (SACCF), as well as due to glacial run off (**Figure 1**). The ACC and its frontal systems exhibit strong intra- and interannual variability which drives variability in the conditions experienced at Shag Rocks and South Georgia (Meredith et al., 2005, Murphy et al., 2007, Boehme et al., 2008, Combes et al., 2023). The region is undergoing rapid climate-driven changes, including in

winds, ocean temperature, acidification, circulation, and sea ice extent and duration (Whitehouse et al., 2008; IPCC, 2019; 2022; Cavanagh et al., 2021; Hogg et al., 2021).

How Patagonian toothfish will be affected by these ongoing changes is uncertain (IPCC, 2019). The life history of this long-lived species (~50 years) includes a prolonged pelagic phase during early development. Eggs and larvae are planktonic in surface waters and therefore may be susceptible to changes in sea surface temperature (SST), which may influence planktonic duration, development rate and survival of eggs and larvae (North, 2002). Following dispersal, larvae settle as small juveniles to demersal habitats in shallow waters with a gradual migration deeper as they grow (Collins et al., 2010). These ontogenetic shifts result in exposure to a range of environmental conditions throughout early life-stages. Retention of eggs and larvae near South Georgia and Shag Rocks is influenced by oceanographic conditions, with prevailing currents likely influencing rates of recruitment to the population (Brigden, 2019). The smallest post-settlement fish in this population (length < 20 cm) are found mainly on the continental shelf around Shag Rocks at depths of 100–300 m (Collins et al., 2007, 2010; Belchier & Collins, 2008), adopting a primarily benthic lifestyle, although smaller individuals may also forage in the water column (Collins et al., 2007). As individuals in this population grow, their range expands as adult toothfish are broadly distributed around the continental shelf margin surrounding South Georgia and Shag Rocks, which may potentially be linked with temperatures near the seafloor (Jones et al., 2025). Spawning occurs annually in austral autumn and winter, typically along the South Georgia–Shag Rocks continental slope (Bamford et al., 2024; **Fig. 1**), likely influenced by oceanographic conditions, including temperature (Everson and Murray, 1999; Boucher, 2018; Brigden, 2017, 2019; Bamford et al., 2024).

Patagonian toothfish are the target species of a valuable deepwater commercial longline fishery that began in the late 1980s (Agnew, 2000; Collins et al., 2010). In South Georgia waters, the fishery is managed within the framework of the Commission for the Conservation of Antarctic Marine Living Resources (CCAMLR) (https://fisheryreports.ccamlr.org/). The stock assessment informing

management of Patagonian toothfish at South Georgia and Shag Rocks is an age-structured model (Earl et al., 2023, Earl & Readdy, 2024, Casal2 Development Team, 2024) which estimates historical abundance and recruitment based on groundfish survey abundance and age composition, tag recapture rates, catch age compositions, catch per unit effort and biological data. Current management is based on a 35-year projection (Constable, 2000) where estimates of historic recruitment are used to inform assumptions in the projection about the level and variability of future recruitment. However, in a variable or changing environment, these baselines may not reliably predict future population dynamics, and do not fully consider changing climate (Cavanagh et al., 2021; Earl et al., 2024; Ouzoulias et al., 2024). Moreover, although changes in distribution and biology are monitored, environmental parameters are not explicitly included in the assessment framework (Welsford et al., 2023). The CCAMLR Workshop on Climate Change (WS-CC-2023, SC-CAMLR-42, Annex 11) resulted in several recommendations directed to CCAMLR's Working Group on Fish Stock Assessment (WG-FSA) in this regard (Cavanagh and Pardo, 2024). WG-FSA has begun to address these, via its work plan, particularly in summarising evidence for changes in stock assessment and population parameters or processes that could be due to the effects of environmental variability or climate change (WG-FSA-IMAF-2024, paragraphs 7.9-7.14, Tables 19-23), including for Patagonian toothfish in Subarea 48.3 (WG-FSA-IMAF-2024, Table 19).

Here, we explore the relationship between Patagonian toothfish and temperature during early life-stages at South Georgia and Shag Rocks, focused on conditions related to abundance of small-sized toothfish (< 26 cm, 26-37 cm), putatively representative of 1 and 2 year-old fish. We consider temporal variation in abundance and investigate the degree to which temperature at different depths during the timing of early development stages, from spawning to benthic settlement, are correlated with abundance. This work provides a foundation for identifying Patagonian toothfish-environment relationships across life-history stages. Understanding these relationships can help determine key factors driving distribution and inter-annual variability in abundance, improving knowledge of climate change effects and informing fisheries management.

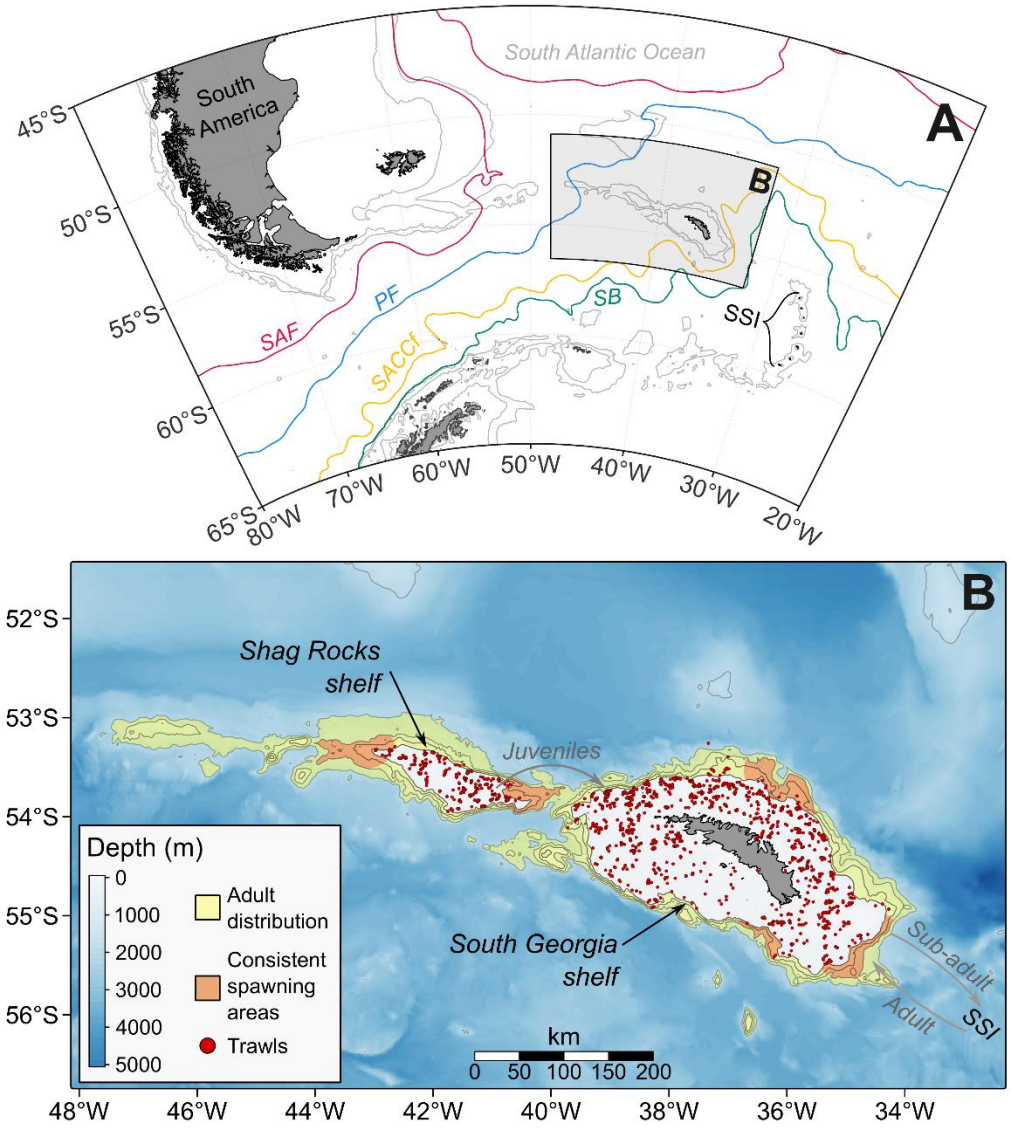

Figure 1. *The location of South Georgia and the surrounding shelf area in the southwest Atlantic are shown in relation to South America (**A**), along with the location of major oceanographic features (SAF = Subantarctic Front, PF = Polar Front, SACCF = Southern Antarctic Circumpolar Current Front, SB = Southern Boundary of Antarctic Circumpolar Current; taken from Park and Durand 2019) and the South Sandwich Islands (SSI) chain. The South Georgia and Shag Rocks shelf are shown in detail (**B**), with information on the distribution of adult toothfish (between 500 and 2000 m isobaths) and known spawning grounds (taken from Bamford et al., 2024), and locations of demersal trawls used throughout analyses. Bathymetry data were sourced from the ETOPO 2022 dataset (NOAA 2022), and contour lines represent 500, 1000, 1500 and 2000 m isobaths (**A**: 500 and 2000 only).*

Methods

Groundfish trawl survey data

Data on Patagonian toothfish distribution and abundance were collected during groundfish surveys conducted approximately biennially on the South Georgia and Shag Rocks shelves between 1986 and 2023 (**Figure 1**; see ***Supplementary materials***, **Table S1**). Sampling methods have been consistent over time, consisting of 30-minute demersal trawls (120-foot otter trawl, 18-20m wingspread, 3-6m headline height, 40 mm cod end mesh; Belchier et al., 2015) at a ship speed of ~3 knots carried out between nautical twilight at dawn and dusk. Surveys were predominantly during the austral summer (November-February), except for 1997 and 2007 (August-September), 2008 (April), and 2021 (May; see **Table S1**). Trawl sampling encompassed the continental shelves of South Georgia and Shag Rocks at depths ranging from 75 to 700 m, although 95% of trawls were at depths less than 330 m. Nearshore and shallower areas (< 100 m), as well as locations directly south of South Georgia, were less frequently sampled due to accessibility and ground suitability (see Hollyman et al., 2021, 2023). For each trawl, total toothfish abundance was recorded as well as mean trawl depth, trawl distance, and horizontal wingspread. In addition, the majority of captured toothfish were measured (total length; cm) and weighed, allowing for the identification of size-distributions and a detailed evaluation of interannual variability in abundance by size-class.

Size distributions and construction of size-classes

Size frequency data were used to identify size-classes, putatively representative of 1 to 6+ (adult) age groups, based on discrete modes represented in size distributions among years (**Table 1**) and guided by known growth rates in juvenile Patagonian toothfish (~100-120 mm per year; Collins et al., 2010). The total number of individuals caught in each trawl within each size-class was then enumerated based on measured size and size-class limits to obtain size-class specific counts for each trawl (**Table 1**). While size class limits were generally applicable across most years, we modified them to account for differences in survey timing, most notably for surveys performed in April-May (2008, 2021), September (1997, 2007), or early December (1987, 1988; **Table S1**), so that single-year cohorts were not divided

among size-classes. Catch per unit effort (CPUE; individuals km^{-2}) was also calculated based on individuals caught per area swept (trawl distance × wingspread; km^2) (Hollyman et al., 2021, 2023). For each size-class we then calculated the mean CPUE per survey, along with its 95% confidence interval via bootstrap resampling (n = 1000 permutations). This was calculated separately for the Shag Rocks and South Georgia shelf areas to investigate changes in abundance through time.

Throughout we refer to these size-classes via the shorthand notation $Sz_{lengths}$, where lengths indicates the length range (total length) in cm included in that size-class. Furthermore, as much of our analysis focuses on abundance of the two smallest size-classes, $Sz_{<26}$ and $Sz_{26\text{-}37}$, we use the term juvenile to refer to these to distinguish them from the remaining size-classes.

***Table 1**. Size-classes applied to Patagonian toothfish (Dissostichus eleginoides) caught in groundfish surveys at South Georgia and Shag Rocks. Ages are based on growth rates in Collins et al. (2010) and are indicative only. Larger size-classes may encompass individuals spanning two or more years of age.*

Size-class	Label	Size range (cm)	Age (years)
1	$Sz_{<26}$	≤ 25	1
2	$Sz_{26\text{-}37}$	26 - 37	2
3	$Sz_{38\text{-}47}$	38 - 47	3
4	$Sz_{48\text{-}57}$	48 - 57	4
5	$Sz_{58\text{-}66}$	58 - 66	5
6	$Sz_{>66}$	> 66	6+

Analyses of temporal variation in abundance of early life-stages at Shag Rocks

For the smallest two size-classes, $Sz_{<26}$ (total length TL < 26 cm) and $Sz_{26\text{-}37}$ (TL = 26-37 cm), putatively representative of age 1 and 2 individuals, respectively, we investigated whether interannual variability in abundance was related to temperature during early development stages. For these analyses we only used trawl data from the Shag Rocks shelf as these size-classes were rarely caught on the South Georgia shelf (2% and 7% of $Sz_{<26}$ and $Sz_{26\text{-}37}$ fish captured; n = 3737 and 2839, respectively); results are therefore only applicable to variation at Shag Rocks. Furthermore, analyses were performed independently for both size-classes, rather than just for the smallest size-class, because catches of $Sz_{<26}$

fish have been near-absent in particular years, despite the occurrence of a strong $Sz_{26\text{-}37}$ size-class in the following year. This discrepancy may arise due to gear selectivity, or because of the more localized and patchy distribution of the smallest size-class (Jones et al., 2025). Performing analyses for both size-classes therefore allowed us to explore relationships between temperature and juvenile abundance, potentially avoiding concerns outlined above, but with the caveat that $Sz_{26\text{-}37}$ fish are older and therefore subject to additional factors that may influence their abundance.

To inform these analyses, daily temperature fields for the study region (50-64°S, 30-50°W) were extracted from two different products available through the Copernicus Marine Service. Sea surface temperature (SST) for the period 1993-2023 was obtained from the Global Ocean and Sea Ice Analysis (OSTIA, https://doi.org/10.48670/moi-00165; Donlon et al., 2012, Good et al., 2020) dataset, and consisted of daily maps at 0.05° resolution. 3D temperature fields for full ocean depth for the years 1993-2023 were obtained from the Global Ocean Physics Reanalysis dataset (GLORYS12V1, https://doi.org/10.48670/moi-00021; Lellouche et al., 2021). GLORYS12V1 has a horizontal resolution of 0.083° with 50 standard vertical levels ranging from 1 m thick in the upper levels to 450 m thick at 5000 m, with seafloor temperature provided as an additional output. GLORYS12V1 is an estimate of the state of the ocean which assimilates ocean observations and has been used in previous studies to examine variability in the marine environment around South Georgia and the South Sandwich Islands where 3D data have been required but observations do not provide sufficient temporal and spatial coverage (Hollyman et al., 2022, Saunders et al., 2022, Thorpe & Murphy, 2022). A comparison of GLORYS12V1 temperature with *in-situ* measurements from a summer survey carried out at South Georgia found that while surface water temperature tended to be overestimated in the GLORYS12V1 output, temperatures at depths below 50 m were generally within ±0.5°C of the observations (Saunders et al., 2022). To further examine the ability of GLORYS12V1 to reproduce the subsurface water properties in our study region in austral winter, we carried out a comparison with additional vertical temperature profile data collected around South Georgia (**Figure S9**). This indicated generally

good agreement in April and July, although the GLORYS12V1 dataset performed less well in September. As such, we treat conclusions based on subsurface temperature relationships with some caution.

Each daily temperature field was cropped to the 1500 m isobath surrounding Shag Rocks and the South Georgia shelf. The fields were divided at 40°W to distinguish conditions at Shag Rocks from those on the South Georgia shelf where juvenile abundance is typically lower, but where adults occupy the shelf edge. Using these data, we calculated annual mean temperature fields during four stages of toothfish early development by averaging across days specific to the following stages: spawning (June-August; Bamford et al., 2024), pelagic eggs (September-November; North, 2002), pelagic larvae (December-February; North, 2002, Belchier and Collins, 2008), and post-larval benthic settlement (March-May). Given differences and uncertainty regarding the depth distribution inhabited during each developmental stage, average temperatures were calculated for several depth strata (summarised in **Table 2**), determined by the vertical distribution of: spawning adults (700-1000 m; Collins et al., 2010); eggs, which rise from ~1000 m potentially to the surface, although few eggs have been captured at South Georgia (7 records at depths of 0-500 m; North et al., 2002); pelagic larvae, which have mostly been caught in the upper water column (23 of 43 larvae caught at depths of 0-3 m, 18 of 43 caught at depths of 3-250 m; North et al., 2002); and post-larval fish following settlement to the benthos (majority at seafloor depths < 250 m; South Georgia groundfish survey dataset). As spawning occurs around South Georgia and Shag Rocks (Bamford et al., 2024), we calculated temperature measures for spawning, egg, and larval stages separately for both South Georgia and Shag Rocks. This was to ascertain which, if any, season by regional division had the strongest correlation with juvenile abundance at Shag Rocks in subsequent years. However, because we only included juvenile abundance from Shag Rocks, we only tested temperature measures from Shag Rocks for the benthic settlement time-window (March to May). Annual temperature measures for each stage were then assigned to surveys and size-classes based on the presumption that $Sz_{<26}$ fish present in January (typical survey timing; **Table S1**) of year Y likely resulted from spawning in June-August of year Y-2, with temperature measures for subsequent developmental stages (egg dispersal, larval dispersal, post-larval settlement)

assigned accordingly. These analyses were limited to groundfish surveys from 1997-2023 (n = 19 surveys), as GLORYS12V1 data used to inform seafloor and midwater temperature covariates were only available from 1993 onwards, which meant that temperature data were only available for surveys after 1995 due to the temporal lags we investigated.

Table 2. *Description of temperature covariates and rationale for their use in analyses of interannual variation in abundance of juvenile Patagonian toothfish at Shag Rocks. For midwater temperatures, exact depth range end points were based on depth limits of the 50 vertical levels within the GLORYS12V1 dataset (https://doi.org/10.48670/moi-00021). Associated depth level numbers for midwater depth strata are given in [].*

Depth strata	Stages	Rationale
Surface: SST	Egg (Sep-Nov) Larvae (Dec-Feb) Settlement (Mar-May)	Temperature potentially experienced by eggs and/or pelagic larvae if within surface mixed layer
Midwater: 110 – 267 m [23-27]	Spawning (Jun-Aug) Egg (Sep-Nov) Larvae (Dec-Feb)	Temperature potentially experienced by eggs and/or pelagic larvae in water column
Midwater: 267 – 454 m [28-30]	Spawning (Jun-Aug) Egg (Sep-Nov) Larvae (Dec-Feb)	Temperature potentially experienced by eggs and/or pelagic larvae in the water column
Seafloor: < 267 m	Spawning (Jun-Aug) Settlement (Mar-May)	Temperature potentially experienced by initially benthic eggs and juveniles following benthic settlement
Seafloor: 644 – 1063 m	Spawning (Jun-Aug)	Temperature potentially experienced by adults and eggs during spawning at depth

Trawl counts for each of the two size classes ($Sz_{<26}$, $Sz_{26\text{-}37}$) were used as the dependent variable representative of abundance in each year, allowing us to control for differences in depth and spatial arrangement of trawls among surveys. For each size-class we fitted a set of Generalised Additive Mixed Models (GAMM; Wood, 2011), all of which included survey random effects, an offset term of swept-area to account for differences in trawl effort and such that fitted models were representative of CPUE, and smooths for depth and spatial variation. Models varied via the inclusion of a smooth term for temperature, with each candidate temperature covariate (**Table 2**) tested in separate models, and a smooth term for date to model a continuous trend:

$$\log(\hat{y}_i) = \log(A_i) + \mu_0 + \alpha_{S_i} + s(D_i) + s(E_i, N_i) + s\left(T_{Y_i}\right) + s(t_{S_i})$$

[eqn. 1]

where $\hat{y}_i$ is the fitted value for trawl *i*, $\log(A_i)$ is an offset term of swept area, μ_0 is the intercept, α_{S_i} are survey random effects, and $s(..)$ are smooth functions specified for trawl depth, D_i, trawl easting, E_i and northing, N_i, coordinates (in km), the date of each survey, t_{S_i}, modelling a continuous trend through time, and temperature, T_{Y_i}, with Y_i indicating the year from which temperature was assigned to a particular survey, dependent on size-class and developmental stage being tested (**Table 2**). Models were fitted assuming that counts, y_i followed a negative binomial distribution (family = nb, log-link):

$$y_i \sim NB\left(\hat{y}_i, \hat{\theta}\right)$$

[eqn. 2]

where $\hat{\theta}$ is the negative binomial dispersion parameter. All smooth functions were thin-plate regression splines (basis = 'tp'), apart from spatial effects that were specified by a two-dimensional Gaussian process smooth (Kammann and Wand 2003; Hefley et al., 2016). We initially explored variations of models containing only survey, depth, and spatial effects to identify an appropriate null model (see ***Supplementary materials***), which was then kept constant across all subsequent models. We then investigated the addition of individual temperature covariates to this null model. These alternate models were compared based on Akaike's Information Criterion (AIC) and predictive accuracy calculated via leave-one-out cross-validation, holding out entire surveys (n = 19), which effectively tests the ability of temperature relationships to predict abundance in an unseen year. Predictive accuracy was quantified using a likelihood-based score (Dormann et al., 2018), equal to the log-likelihood of the held-out data given predictions from the model trained on the remaining data. For interpretability, we converted scores to a measure akin to deviance explained:

$$pD_{mod} = \frac{\mathcal{L}_{null} - \mathcal{L}_{mod}}{\mathcal{L}_{null} - \mathcal{L}_{best}}$$

[eqn. 3]

where $\mathcal{L}_{mod}$ and $\mathcal{L}_{null}$ are the cross-validated likelihood scores (lower = lower prediction error) of the focal model and null model, respectively, and $\mathcal{L}_{best}$ is the likelihood of a model where all interannual variability is explained (see ***Supplementary materials***). The resulting measure varies from 0, where the model performs no better than the null model and explains no interannual variation, to 1 where model predictions are as good as possible within the constraints of explaining interannual variability. All GAMMs were fitted using the gam function in the mgcv package in R (Wood 2011).

Analyses of long-term temperature trends

To supplement these analyses, we also tested for long-term trends in surface, sub-surface (depth: 110-267 m) and seafloor temperatures during spawning (June-August), egg (September-November), larval (December-February) and post-larval settlement (March-May) developmental stages. For each temperature metric, trends through time were estimated by fitting a linear model with year as the independent variable using Generalised Least Squares (GLS, package nlme; Pinheiro et al., 2025) with a first-order autoregressive correlation structure (AR1) to account for temporal autocorrelation. We present results regarding long-term trends via the estimated mean trend coefficient, expressed as degrees C per decade, along with 95% confidence interval.

Exploration of water column temperature variability in relation to juvenile abundance

Following the analyses relating interannual variability in juvenile abundance to temperature, we then explored differences in temperature throughout the water column during the spawning period (June to August) between years of low juvenile abundance versus moderate-high juvenile abundance. This characterisation was based on putative year-class strength indicated by CPUE on the Shag Rocks shelf for the $Sz_{<26}$ and $Sz_{26\text{-}37}$ size-classes. For each year of available data (n = 26), we characterised year-

class strength as either moderate-high versus low, using the lower quartile of year-averaged CPUE at Shag Rocks as the cut-off, such that low years were those where CPUE was below the 25th percentile of CPUE among all years. This was performed independently for $Sz_{<26}$ and $Sz_{26\text{-}37}$ size-classes because each potentially provides information on conditions 1 and 2 years prior to the survey, respectively, enabling us to infer conditions for a greater number of years given the typical biennial timing of groundfish surveys.

We then identified the putative spawning time-period associated with each year-class (Jun-Aug, which we assume were 1.5 and 2.5 years prior to the survey for $Sz_{<26}$ and $Sz_{26\text{-}37}$ fish, respectively) and labelled the spawning period according to year-class strength (low versus moderate-high). Cases where spawning periods were classified by CPUE for both juvenile size-classes (surveys separated by 1 year; n=12) agreed in 7 of the 12 cases, with the remainder being predominantly those where the $Sz_{<26}$ classification was ranked as low and the $Sz_{26\text{-}37}$ classification ranked as moderate (**Table S5**). In those instances, we defaulted to the $Sz_{26\text{-}37}$ classification of year-class strength given concerns raised earlier regarding the consistency of sampling for the $Sz_{<26}$ size-class. As survey-averaged CPUE might be biased by the spatial and depth distribution of trawls on any given survey, we also compared the classifications of year-class strength based on CPUE to those derived from year random effects (α_{S_i}) extracted from a model containing relationships to account for depth ($s(D_i)$) and spatial effects ($s(E_i, N_i)$) fitted to trawl counts of toothfish:

$$\log(\hat{y}_i) = \log(A_i) + \mu_0 + \alpha_{S_i} + s(D_i) + s(E_i, N_i)$$

[eqn. 4]

where the model was fitted to size-class specific counts (y_i) using a GAMM (family = negative binomial, fitted using gam in the mgcv package in R; Wood 2011), with all terms as defined for equation 1. The same process of classifying year-class strength was then applied but replacing survey-averaged CPUE with estimated year random effects (α_{S_i}). Both approaches produced similar classifications of year-class strength (see ***Supplementary materials***).

We then examined water column temperature characteristics during the spawning period (June to August) averaged across years according to year-class strength. Daily temperature fields were extracted from GLORYS12V1 as before and then explored using two different approaches: i) north-south 3D transects of temperature (0-650 m) across the Shag Rocks shelf (52.5-54°S, 41.5°W); ii) horizontal maps of temperature at 110-131 m depth for the South Georgia and Shag Rocks region. This latter dataset corresponds to temperature at or below the mixed layer (typically 100-150 m during June-August in the vicinity of South Georgia; Dong et al., 2008) and lies just above much of the Shag Rocks shelf. In each case, the extracted data (daily; June to August) were averaged over time and over the years as classified based on year-class strength to ascertain average water column conditions associated with low juvenile abundance versus moderate-high abundance.

All analyses and data processing were performed in R version 4.3.3 (R Core Team 2024).

Results

Size distributions and interannual variability

Size distributions of Patagonian toothfish captured in groundfish surveys were indicative of sporadic pulses of juvenile fish at Shag Rocks, with $Sz_{<26}$ cohorts present in seven of the ten surveys from 1987 to 2003, followed by an absence until 2019 (**Figure 2**). However, $Sz_{26\text{-}37}$ fish were present in years between 2004 and 2019 (i.e., 2006, 2010, 2012; **Figure 2**), confirming concerns raised earlier regarding sampling bias for the smallest size-class. Strong cohorts were frequently present in sequential survey years, with particularly dominant cohorts first detected in 1990, 2003, 2010, and 2019 forming the majority of fish captured on the Shag Rocks shelf over the following 2-5 years (**Figure 2**). However, while year-classes were often initially distinct, widening size distributions and overlapping size among year groups prevented identification of individual cohorts for fish larger than ~55-60 cm. In comparison to Shag Rocks, juvenile fish ($Sz_{<26}$ and $Sz_{26\text{-}37}$) were rarely captured on the South Georgia shelf, with CPUE of the $Sz_{<26}$ and $Sz_{26\text{-}37}$ size-classes frequently more than 1-2 orders of magnitude higher on the

Shag Rocks shelf compared to the South Georgia shelf (**Figure 2**). Size distributions on the South Georgia shelf were dominated by larger-sized individuals (median = 53 cm, compared to 42 cm on the Shag Rocks shelf), and lacked the visible cohorts present on the Shag Rocks shelf (**Figure 2**). The difference in CPUE between Shag Rocks and South Georgia decreased with each increase in size-class, with CPUE being almost equivalent between the two shelf locations for the largest size class (> 66 cm), consistent with dispersal toward the South Georgia shelf (**Figure 2**).

Survey-averaged CPUE of the $Sz_{<26}$ size-class on the Shag Rocks shelf varied by more than three orders of magnitude among years, varying from an unusually high value of 9000 individuals km^{-2} in 1990 to zero in multiple years between 2004 and 2017 (**Figure 2**). While CPUE for this size-class appears to have increased in recent years (1999-2023), values remain lower than those typically observed prior to 2000 (**Figure 2**). Broadly similar patterns were observed on the South Georgia shelf (**Figure 2**). Average CPUE of the Sz_{26-37} size-class at Shag Rocks varied less among surveys, and prior to 2006 exceeded 100 individuals km^{-2} in the majority (8 of 12) of years (**Figure 2**). From 2006 onwards, CPUE alternated between periods of low CPUE (2007-2009, 2013-2021) followed by periods of CPUE similar to those recorded prior to 2006 (2010-2012, 2023; **Figure 2**); this pattern was also evident in the Sz_{38-47} size-class on the Shag Rocks shelf, albeit delayed by 1 year. The 2023 survey recorded the highest CPUE of Sz_{26-37} and Sz_{38-47} fish in more than a decade across both shelf locations (**Figure 2**).

For larger size classes (48-57 cm, 58-66 cm, > 66 cm) CPUE has been broadly consistent through time at Shag Rocks (**Figure 2**). However, CPUE of Sz_{48-57} and Sz_{58-66} size-classes at South Georgia decreased from 2009 onwards (mean CPUE 2009-2019 = 1.7 and 1.9 individuals km^{-2} for Sz_{48-57} and Sz_{58-66}, respectively) compared to the previous 10-years (mean CPUE 1998-2008 = 7.3 and 7.1 individuals km^2), which matches the 2007 transition observed in the Sz_{26-37} size-class observed at Shag Rocks (**Figure 2**). However, lower interannual variability of CPUE for the larger size-classes suggest that relative abundance of adults may be buffered from the variability in juvenile abundance.

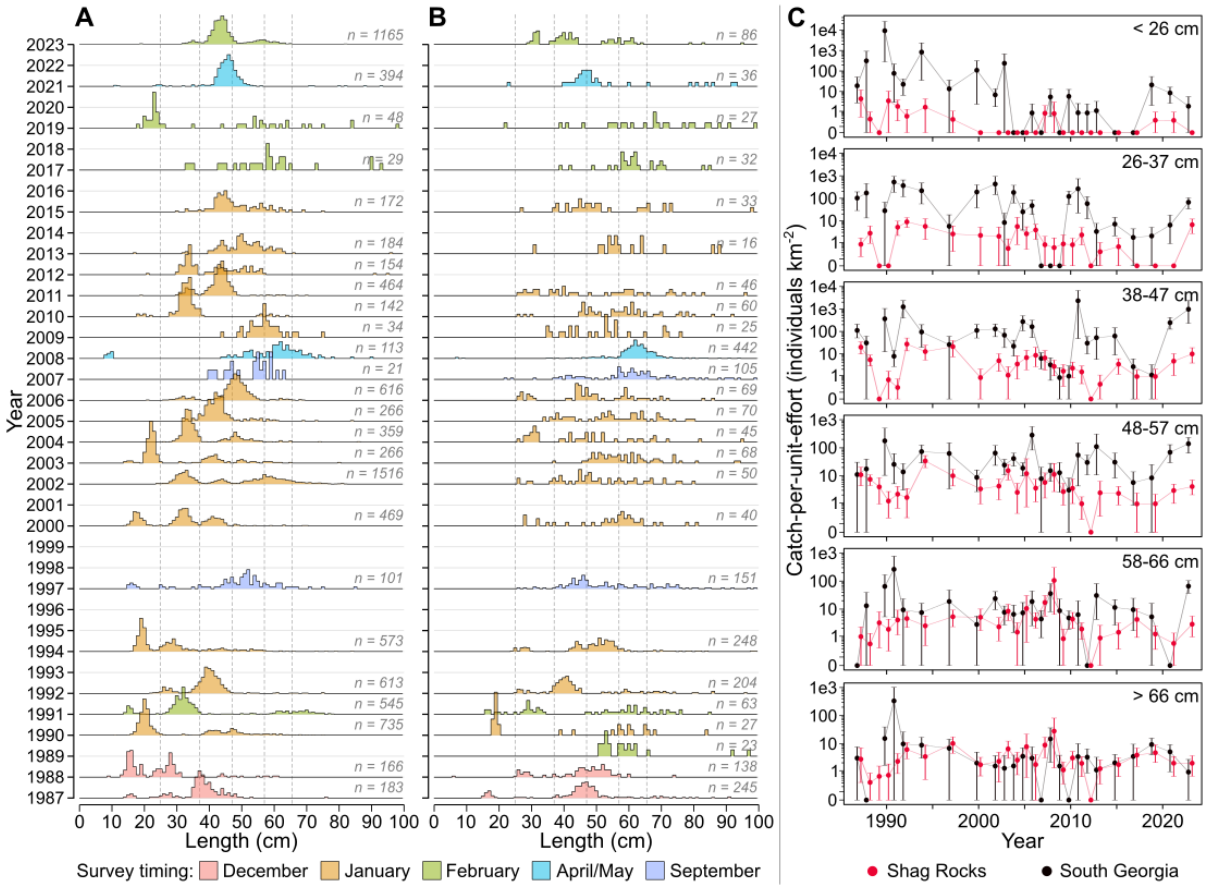

Figure 2. *Size distributions of Patagonian toothfish (Dissostichus eleginoides) caught on the Shag Rocks (**A**) and South Georgia (**B**) shelves during groundfish surveys from 1987 to 2023, along with survey averaged catch-per-unit-effort (CPUE; individuals per km^2) for different size-classes (**C**; < 26 cm, 26-37 cm, 38-47 cm, 48-57 cm, 58-66 cm, > 66 cm) based on total length. Note that histogram heights in (**A**) and (**B**) are scaled according to the total number caught within each survey, provided in grey text to the right of each panel, and therefore represent relative, rather than absolute, abundance in a particular survey. Histograms are colour-coded according to the month in which the majority of trawls were performed in a given survey. Size-class thresholds are indicated by dashed vertical lines in (**A**) and (**B**). Values in (**C**) correspond to the survey-mean CPUE calculated according to counts of individuals caught within each size-class divided by trawl swept area (km^2). Error bars indicate the bootstrapped 95% confidence interval of the mean.*

Abundance of early life-stages in relation to environmental variability

Size: < 26 cm

Models fitted to annual abundance of $Sz_{<26}$ fish on the Shag Rocks shelf suggest a positive correlation with temperature during egg and larval dispersal phases, irrespective of the depth at which temperature was assessed (surface or midwater; **Figure S2**), but no relationship with temperatures during spawning (**Figure 3**). The temperature covariate with the highest predictive accuracy was that calculated in midwater over the Shag Rocks shelf during egg dispersal (predictive accuracy score, pD = 0.69, indicative of 69% of interannual variability explained by temperature; **Table 3**), and was suggestive of a 10-fold increase in abundance with temperature increasing from 1.4°C to 1.8°C (**Figure 3**). Surface temperatures during the larval-dispersal period and seafloor temperatures during the benthic settlement stage were also positively correlated with abundance but had lower predictive accuracy (**Table 3**). Inclusion of a continuous trend through time had no impact on which temperature effects were identified as important (**Table 3**), but when included by itself indicated a declining trend in abundance from 1997 to 2010, followed by an increasing trend from 2015 to 2023 (**Figure S2**). Fitted spatial effects also suggested a highly constrained distribution on the Shag Rocks shelf largely due to depth range (depth < 200 m; **Figure S3**).

Size: 26-37 cm

Similar to results found for $Sz_{<26}$ fish, models fitted to abundance of the 26-37 cm size-class on the Shag Rocks shelf were also indicative of a positive correlation with temperature during the egg dispersal stage (**Figure 3D**). However, the strongest relationship for this size-class came from models containing temperatures calculated during the spawning time-window (June-August) over the Shag Rocks shelf either at the seafloor (seafloor depth < 267 m, pD = 0.69) or in the midwater column at 110-267m depths (pD = 0.45; **Table 3**). The fitted relationship between abundance and temperature during spawning indicated that abundance increases with temperature up to a maximal value at temperatures of 1.65°C (seafloor temperature; **Figure 3C**) or 1.9°C (midwater temperature; **Figure S4**) and then declines at higher temperatures. Models containing temperature covariates assessed during larval-dispersal or settlement stages performed worse than the null model, indicating weak to no effect.

Although including a continuous trend through time indicated an overall declining trend in abundance of $Sz_{26\text{-}37}$ fish (**Figure S4**), models containing this term had lower predictive accuracy both when included alone (pD = -0.02; **Table S3**), or when included with temperature covariates (reduction in pD relative to equivalent models of 0.04-0.13; **Table 3**). This may suggest that long-term patterns are more strongly characterised by fluctuations in abundance among years, or groups of years, rather than by a continuous trend through time. Fitted spatial effects for the 26-37 cm size-class indicated a deeper and more widespread distribution across the Shag Rocks shelf compared to that found for the < 26 cm size-class (**Figure S5**), consistent with an ontogenetic shift toward deeper areas as toothfish grow.

Table 3. *Summary statistics for models fitting abundance of < 26 cm and 26-37 cm Patagonian toothfish on the Shag Rocks shelf to temperature conditions during different early development stages (Spawn = Jun-Aug, Egg = Sep-Nov, Larvae = Dec-Feb, Settlement = Mar-May), locations (SR = Shag Rocks, SG = South Georgia), and depth strata. Statistics shown are the model estimated degrees of freedom (edf), Akaike's Information Criterion (AIC), deviance explained (D^2), and predictive deviance score (pD) calculated via cross-validation. The Date column indicates whether models also included a continuous trend through time. Only those models that improved on the null model (based on predictive scores) are presented; see* ***Table S3-S4*** *for all model statistics.*

Stage	Area	Depth	Date	edf	AIC	D^2	pD
Length: < 26 cm							
NULL				21.9	316.8	79.8	0.00
Egg (Sep-Nov)	SR[a]	Midwater (110-267 m)		20.0	315.8	79.1	0.69
Larvae (Dec-Feb)	SR[a]	Midwater (110-267 m)		20.5	318.9	78.4	0.65
Larvae (Dec-Feb)	SG[b]	Surface		22.6	317.6	79.9	0.27
Settlement (Mar-May)	SR	Seafloor (< 267 m)		22.4	319.2	79.4	0.37
NULL			Y	21.5	316.6	79.6	0.24
Spawn (Jun-Aug)	SG	Seafloor (< 267 m)	Y	21.7	316.8	79.7	0.28
Egg (Sep-Nov)	SR	Midwater (110-267 m)	Y	20.9	317.5	79.1	0.63
Larvae (Dec-Feb)	SR[a]	Surface	Y	21.9	317.8	79.5	0.48
Larvae (Dec-Feb)	SG[b]	Midwater (110-267 m)	Y	20.3	316.7	78.9	0.64
Length: 26-37 cm							
NULL				23.1	1029.7	58.9	0.00
Spawn (Jun-Aug)	SR[a]	Midwater (110-267 m)		22.5	1028.3	59.0	0.45
Spawn (Jun-Aug)	SR	Seafloor (< 267 m)		21.8	1027.8	58.8	0.69
Egg (Sep-Nov)	SG[b]	Midwater (110-267 m)		22.8	1028.8	59.0	0.21
Larvae (Dec-Feb)	SG	Midwater (110-267 m)		23.1	1029.6	59.0	0.16
NULL			Y	23.3	1030.2	58.9	-0.02
Spawn (Jun-Aug)	SR	Midwater (110-267 m)	Y	22.5	1028.1	59.0	0.32
Spawn (Jun-Aug)	SR	Seafloor (< 267 m)	Y	22.1	1028.0	58.9	0.65
Spawn (Jun-Aug)	SG[b]	Seafloor (644-1063 m)	Y	23.2	1029.7	59.0	0.13
Egg (Sep-Nov)	SR	Midwater (110-267 m)	Y	22.8	1028.5	59.0	0.09

[a]: Temperatures at South Georgia for this season and depth also performed better than the null, but had higher predictive likelihood scores and displayed similar fitted temperature effects

[b]: Temperatures at Shag Rocks for this season and depth also performed better than the null, but had higher predictive likelihood scores and displayed similar fitted temperature effects

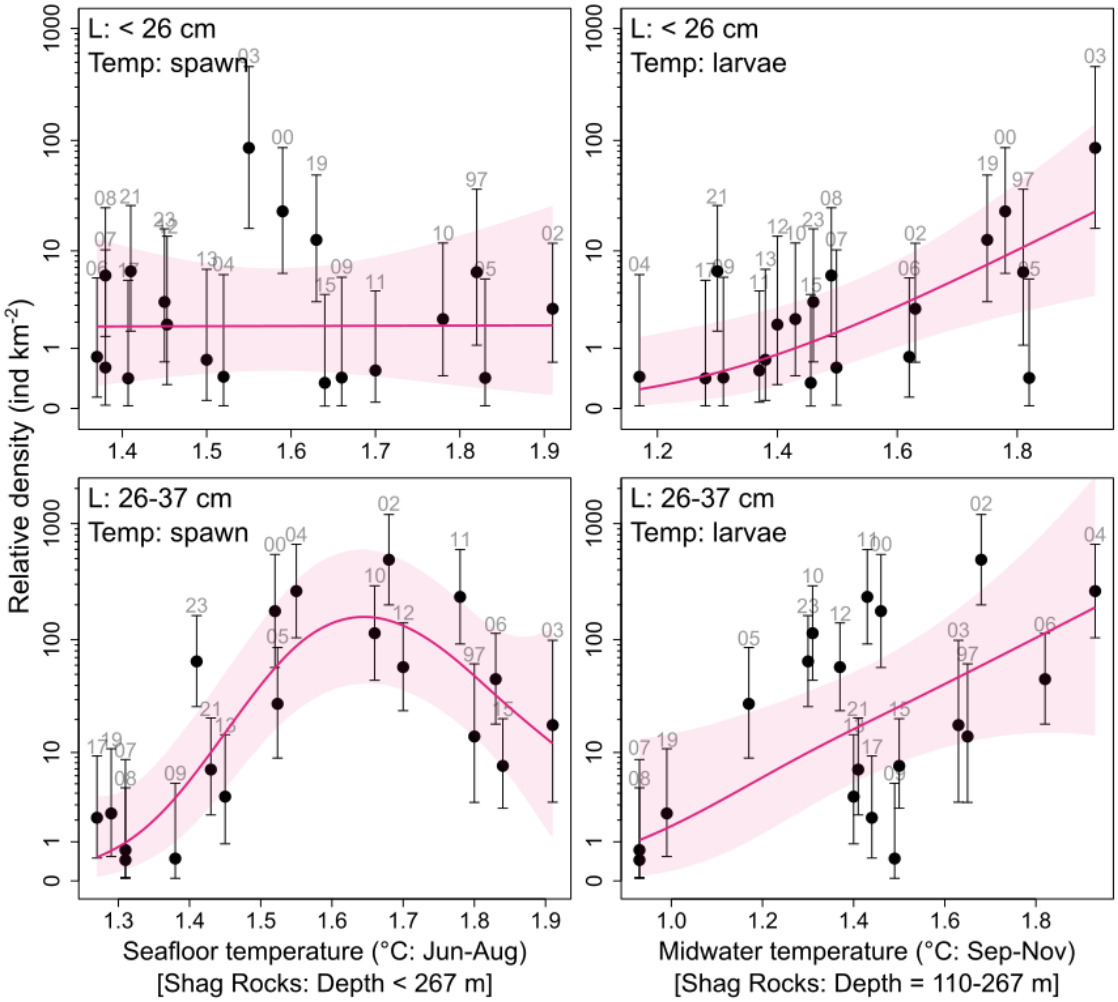

Figure 3. *Fitted relationships between observed catch-per-unit effort (CPUE; individuals km^{-2}) of juvenile Patagonian toothfish (Dissostichus eleginoides) on the Shag Rocks shelf and temperature during different stages of early development. Panels correspond to relationships for < 26 cm (upper) and 26 – 37 cm (lower) size-classes for the two temperature covariates that were the best predictors of annual abundance: seafloor temperature on the Shag Rocks shelf calculated during spawning (June-August, left panels), and midwater temperature at 110-267 m calculated during egg-dispersal (September-November, right panels). Points and error bars are the mean (± 95% confidence interval) predicted density for a given survey from the null model after accounting for depth and location effects for each size-class. Lines and shading indicate the fitted relationship and 95% CI from the model fitted with the corresponding temperature effect.*

Long-term trends in temperature specific to stages of early development

Given the importance of temperatures on the Shag Rocks shelf at various stages throughout early development of Patagonian toothfish, we chose to examine long-term trends in seafloor, midwater (or subsurface; 110-267 m depth), and sea surface temperature during each of the putative spawning, egg, larval, and post-larval benthic settlement stages (**Figure 4**). Long-term trends over a 30-year time-period during spawning (June-August) and egg (September-November) stages were indicative of warming in the surface layers, and a contrasting cooling trend in subsurface and seafloor temperatures (**Figure 4**. Surface warming was greatest during the egg dispersal time-window, having increased at an average rate of 0.23°C/decade, whereas trends of subsurface cooling were strongest during spawning (-0.1 °C/decade; **Figure 4**). Long-term patterns of temperature during larval (December-February) and benthic settlement (March-May) stages indicated no trend over the same time-period for all depth levels, except for surface temperatures during December-February, which displayed an increasing trend of 0.11°C/decade, albeit with high interannual variability (**Figure 4**). Collectively, these trends indicate that temperature conditions have changed the most during the spawning and egg-dispersal stages of Patagonian toothfish at South Georgia but have remained approximately constant over time for the latter developmental stages.

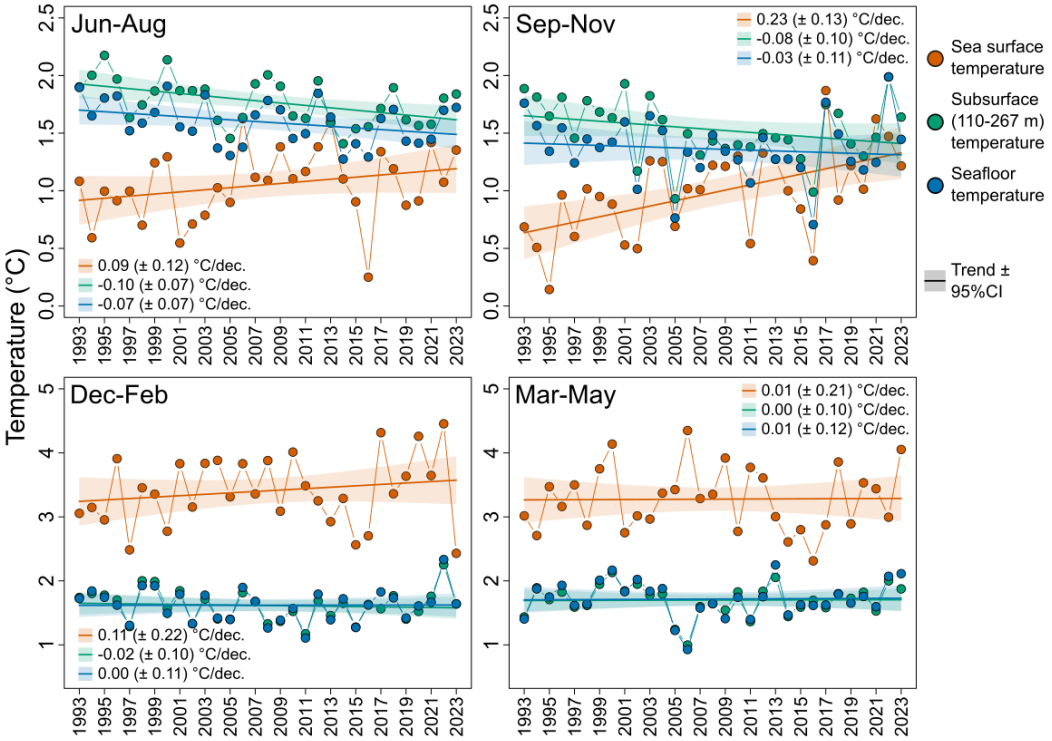

Figure 4. *Long-term trends in temperature over the Shag Rocks shelf by time-period and water column strata (sea surface, subsurface, seafloor) specific to early development of Patagonian toothfish (Dissostichus eleginoides). Panels correspond to seasonal average temperatures calculated per year for June-August, September-November, December-February, and March-May, putatively representative of spawning, egg, larval, and post-larval stages of toothfish in the South Georgia and Shag Rocks region, respectively. Subsurface (depth = 110-267 m) and seafloor (depth < 267 m) temperature data were extracted from the Global Ocean Physics Reanalysis dataset, whereas sea surface temperature were obtained from the Global Ocean OSTIA dataset, both archived on the Copernicus Marine Data Store. Trend lines are those from a linear model fitted to the corresponding data, with shading to indicate the 95% confidence interval. Trend estimates, and 95% CI are also given as °C/decade.*

Exploration of water column temperature variability in relation to juvenile abundance

Prior to years with low juvenile abundance (abundance of the $Sz_{<26}$ or $Sz_{26\text{-}37}$ size-class at or below the lower quartile across available years), average temperatures during spawning were characterised by a deeper transition from cold surface waters (< 1.4°C) to warmer subsurface waters (typically > 2°C) when compared to years in which juvenile abundance was high (**Figure 5**). In years preceding high

juvenile abundance, warmer water conditions (> 1.5°C) prevailed on and above the seafloor at the Shag Rocks shelf, while the same locations were 0.3 to 0.4°C colder in years of low juvenile abundance (**Figure 5**). Temperatures at a depth of 110-131 m were uniformly colder in poor spawning years relative to normal throughout the South Georgia region. Furthermore, warmer water at depths of 100-200 m that typically covers the Shag Rocks shelf in years of good recruitment was absent in poor years, with warmer subsurface conditions shifted westward off the Shag Rocks shelf (**Figure 5**).

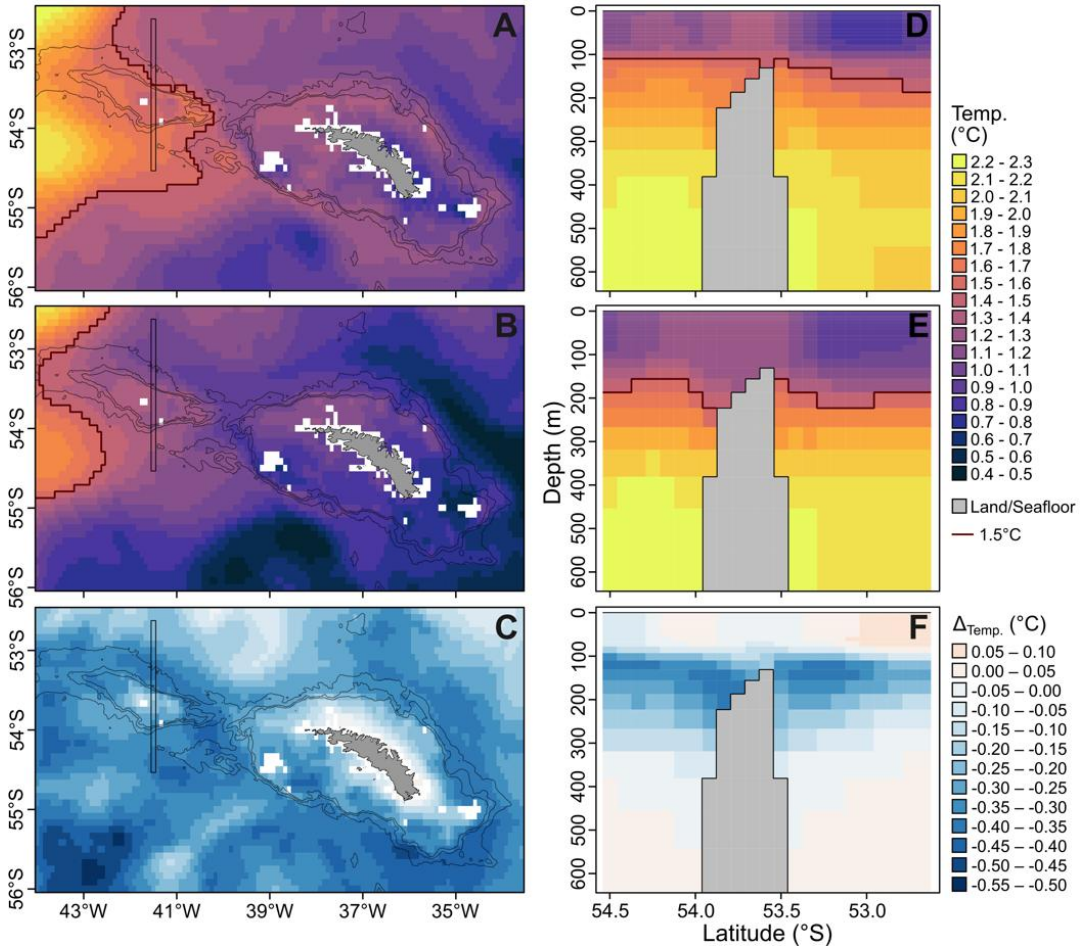

Figure 5. *Temperature at depth averaged across years during the Patagonian toothfish (Dissostichus eleginoides) spawning season (June-August). Panels correspond to the average water temperature at 110-131 m throughout the South Georgia region (**A** and **B**), and for a cross-section (vertical black rectangle in **A** and **B**) spanning the Shag Rocks shelf (**D** and **E**) showing temperature variation according to depth and latitude. Alternate maps and cross-sections correspond to temperatures averaged over years in which juvenile toothfish abundance was moderate to high (**A** and **D**; years = 1995-2003, 2007-2009, 2011, 2017, 2019-2021) versus low (**B** and **E**; years = 2004-2006, 2010, 2012-2016, 2018) based on catch-per-unit effort (CPUE) on the Shag Rocks shelf during groundfish surveys.*

*The difference in temperature maps (**C**) and cross-sections (**F**) between the two year-sets is also shown (low minus moderate to high)*.

Discussion

This study examined Patagonian toothfish populations in the context of their variable and changing environment, focusing on key habitat for juvenile fish around South Georgia and Shag Rocks. Over the past 30 years, surface waters in the region have warmed, while subsurface and seafloor layers have shown cooling trends, highlighting complex vertical temperature dynamics. We integrated almost three decades of groundfish survey data with ocean temperature records throughout the water column to explore how environmental conditions may influence Patagonian toothfish populations. The analysis revealed significant interannual variability in juvenile Patagonian toothfish abundance, with strong correlations to temperature dynamics during early life stages. These findings offer new insight into how long-term environmental change and short-term variability may be influencing recruitment patterns and population dynamics in this system.

Our findings reinforce the importance of the Shag Rocks shelf to early life stages (Collins et al., 2007; Belchier & Collins, 2008) and demonstrate strong interannual variability in smaller size-classes of Patagonian toothfish, with multi-year periods of alternating high and low abundance, and an apparent slight long-term decline in abundance of juvenile fish. This strong interannual variability was not evident in the larger size-classes we investigated (> 48 cm), suggesting that populations of sub-adults and adults that remain on the South Georgia or Shag Rocks shelf (within the extent of groundfish surveys) may be buffered to some extent against large changes in juvenile recruitment between years. This may be due to limited on-shelf resources supporting a relatively constant population of larger fish, with density-dependent mortality and off-shelf dispersal (Collins et al., 2010), regulating the population towards carrying capacity. Furthermore, our results indicate that strong year-classes tend to persist, dominating size-distributions at least for the first three years following settlement, which may reduce the impact on the overall population of poorer recruitment in intervening years. However,

consecutive weak cohorts may exceed this buffering capacity, leading to a decline in overall population size.

We found positive relationships between juvenile Patagonian toothfish abundance and temperature, suggestive of greater abundance following warmer conditions, consistent with the broader distribution of this species (Collins et al., 2010). The strongest temperature-abundance relationships were found in the water column, below the surface mixed layer, for both $Sz_{<26}$ and $Sz_{26\text{-}37}$ size-classes. This signal was most pronounced for time lags corresponding to early developmental stages, especially spawning and egg dispersal, which also coincide with times of year that have experienced the greatest temperature changes over the past 30 years.

However, different temperature relationships were found for analyses based on abundances of the smallest size-class, which displayed a simple positive relationship with temperature during egg-dispersal, while abundances of the 26-37 cm fish displayed a more complex modal relationship, with highest abundances coinciding with seafloor/midwater temperatures of 1.6-1.9°C during spawning. In addition, the overall strongest relationship, across size-classes and temperature covariates, was for abundances of 26-37 cm fish in relation to temperatures during spawning, despite the longer time-lag (2.5 years) compared to that evaluated for the < 26 cm size-class. A potential explanation for this discrepancy relates to the reliability of CPUE of the smallest size-class, with regards to gear selectivity and their patchier distribution, which may act to obscure relationships in relation to environmental variability.

The strong relationship found between CPUE of the 26-37 cm size-class on the Shag Rocks shelf and seafloor/subsurface temperatures during spawning leads to several connected hypotheses. The first is that subsurface temperature influences prey conditions around Shag Rocks for larval or post-larval fish and thereby regulates their abundance via prey limitation under certain temperature regimes. Examination of CPUE of 26-37 cm and 38-47 cm size-classes of toothfish on the Shag Rocks shelf in relation to abundance of yellowfin notothen (*Patagonotothen guntheri*), a primary prey species for

juvenile Patagonian toothfish on the Shag Rocks shelf and that are also recorded during groundfish surveys (Collins et al., 2008), suggests only a weak positive correlation (**Figure S10**) with abundance of the larger 38-47 cm size-class, but no correlation with abundance of the 26-37 cm size-class. However, reduced abundance of yellowfin notothen from 2007 to 2009 was also accompanied by a transition from years of moderate abundance of $Sz_{26\text{-}37}$ and $Sz_{38\text{-}47}$ toothfish, to multiple years (2008-2010) of reduced abundance, suggestive of a common or related mechanism. Notably, this time-period was also accompanied by a shift in seafloor temperatures towards colder conditions on the Shag Rocks shelf that began in 2005 (**Figure 5**), which may have directly impacted both species (distribution of *P. guntheri* is restricted to the Shag Rocks shelf, potentially due to low temperature tolerance; Collins et al., 2008) or via changes to prey community composition important to both yellowfin notothen and juvenile Patagonian toothfish. Further work is required to improve understanding of potential changes to the prey field and corresponding toothfish responses (Ward et al. 2025).

Temperature may also have a direct effect on egg survival and development in Patagonian toothfish, as seen in other species (e.g. Tsoukali et al., 2016), with cooler subsurface conditions during the spawning season potentially leading to higher egg mortality or delayed development. The indication of a deeper thermocline and cooler subsurface conditions during the spawning season prior to low recruitment years suggest that eggs traversing the water column in those years could experience a more extreme change in temperature at greater depths (**Figure 5**). Additionally, these eggs may then occupy cooler water for a period of time, which could delay or inhibit their development. However, this is predicated on eggs remaining at depths below the mixed layer (100-300 m) for a duration sufficient to affect development. The depth distribution of toothfish eggs at South Georgia is poorly understood, and few studies have captured eggs or larvae despite pelagic sampling (North 2002), suggesting that they are either patchily distributed, exhibit net avoidance (larvae), or are present deeper than is typically sampled during pelagic trawls. Evseenko et al., (1995) reported captures of seven eggs in September-October in the upper 500 m of the water column to the north of South Georgia, suggestive of a pelagic distribution. However, North (2002) and Zhivov & Krivoruchko (1990)

have presented arguments that eggs are initially demersal, with the former based on absence of eggs in pelagic sampling despite high abundance calculated from population fecundity. An initially demersal distribution would align with our findings that indicate the importance of seafloor and subsurface temperatures during the spawning and egg dispersal stages to abundance of juvenile toothfish. Improved data on the depth distribution of eggs is essential as vertical position in the water column strongly influences exposure to temperature, currents, and other environmental drivers.

Thus, temperature at Shag Rocks appears to be an important factor for juvenile recruitment, with warmer temperatures below the mixed layer during spawning showing the strongest correlation with juvenile abundance in subsequent years. This is suggestive of lower abundance following spawning periods characterised by cooler temperatures. Notably, while we found that SST at Shag Rocks has increased at a rate of 0.09°C per decade in recent years, sub-surface temperatures, including seafloor temperatures here during the spawning period, the depth and time most indicative of recruit abundance, have decreased by 0.1°C per decade from 1993 to 2023 (**Figure 4**). This may help explain the apparent decline in juvenile abundance. However, while the SST trends are derived from a satellite product and are comparable with the rates calculated from in situ data by Whitehouse et al., (2008), we note that much of our analyses utilised subsurface temperatures taken from a global ocean reanalysis (GLORYS12V1). While multiple observational datasets are assimilated in the reanalysis, the representation of properties including temperature in the reanalysis is affected by the availability of the assimilated in situ data (Lellouche et al., 2021), which may affect the trends reported here.

Given the complex life history of Patagonian toothfish, their important role in the South Georgia ecosystem and the rapid environmental changes in the region, ensuring their sustainable management in the face of future change is essential. Our findings emphasise the importance of considering subsurface thermal structure as well as surface temperature change when evaluating the effects of climate change on Patagonian toothfish (Azarian et al. 2022; Ward et al. 2025). The same would apply for other deepwater species particularly those whose eggs and larvae traverse the water column.

Changing vertical temperature profiles may expose eggs and larvae to conditions that exceed their physiological tolerances. The presence of steep or irregular thermal gradients, such as the transitions described in this study from warmer sea floor temperatures through cooler mid-water to warmer surface temperatures, may be particularly consequential. These vertical gradients could play a significant role in influencing early life stage development, vertical positioning, and survival probabilities, with the potential for effects to be carried forward throughout the life cycle. A further consideration is that model simulations of transport and retention of early life stages of Patagonian toothfish have suggested that variability in local ocean circulation affects their retention in the vicinity of South Georgia and Shag Rocks (Brigden, 2019). Combining model experiments that include temperature effects with dispersal would be a useful next step to better understand recruitment variability.

This study highlights the need for detailed consideration of environmental conditions across key developmental windows to more fully understand species-environment relationships. Such insights would enable future recruitment assumptions used in management to be based on an understanding of the underlying processes, rather than empirical approaches (Alewijnse et al., 2025, Dunn, 2025), thereby enhancing their ecological realism and supporting more climate-responsive management approaches.

Acknowledgements

We acknowledge the UK Government Darwin Plus Programme for funding this project, also the British Antarctic Survey (BAS) and Cefas for providing additional support. RC, MC, JF, SH, ST, CW were additionally supported by the BAS National Capability Antarctic Logistics and Infrastructure program "Research, Conservation and Leadership in Southern Ocean Ecosystems (CONSEC)", supported by the Natural Environment Research Council, a part of UK Research and Innovation. This study was conducted using E.U. Copernicus Marine Service Information (OSTIA sea surface temperature,

https://doi.org/10.48670/moi-00165; GLORYS12V1 full depth temperature; https://doi.org/10.48670/moi-00021).

References

Agnew, D.J., 2000. The illegal and unregulated fishery for toothfish in the Southern Ocean, and the CCAMLR catch documentation scheme. Marine Policy 24(5): 361-374. https://doi.org/10.1016/S0308-597X(00)00012-9

Alewijnse, S.R., Readdy, L., and Earl. T. 2025. Recruitment assumptions in integrated assessments of toothfish. CCAMLR WG-SAM-2025/27

Arkhipkin, A.I., Brickle, P., Lee, B., Shaw, P.W., and McKeown, N.J. 2022. Taxonomic re-appraisal for toothfish (Dissostichus: Notothenioidea) across the Antarctic Polar Front using genomic and morphological studies. Journal of Fish Biology 100(5): 1158-1170. https://doi.org/10.1111/jfb.15013

Azarian, C., Bopp, L., and d'Ovidi, F. 2022. Climate change patterns in the Southern Indian Ocean: warming and marine heatwaves. CCAMLR Working Group on Ecosystem Monitoring and Management WG-EMM-2022/12.

Bamford, C., Hollyman, P.R., Abreu, J., Darby, C., and Collins, M.A. 2024. Spatial, temporal, and demographic variability in Patagonian toothfish (Dissostichus eleginoides) spawning from twenty-five years of fishery data at South Georgia. Deep-Sea Research Part I. 203, 104199. doi.org/10.1016/j.dsr.2024.104260

Belchier, M., and Collins, M.A. 2008. Environmental drivers of recruitment and growth variability in Patagonian toothfish (Dissostichus eleginoides) at South Georgia. Marine Biology. 155: 493-503. https://doi.org/10.1016/j.ecss.2021.107473

Belchier. M., Featherstone, L., and Oliver, J. 2015. Configuration of the FP-120 net used on UK groundfish surveys in CCAMLR Subarea 48.3 (South Georgia). CCAMLR Working Group on Fish Stock Assessment WG-FSA-15/26.

Boehme, L., Meredith, M.P., Thorpe, S.E., Biuw, M., and Fedak M. 2008. Antarctic Circumpolar Current frontal system in the South Atlantic: Monitoring using merged Argo and animal-borne sensor data. Journal Geophysical Research (113), C09012, doi:10.1029/2007JC004647

Boucher, E.M., 2018. Disentangling reproductive biology of the Patagonian toothfish *Dissostichus eleginoides*: skipped vs obligatory annual spawning, foraging migration vs residential life style. Environmental Biology of Fishes 101 (9), 1343-1356. doi: 10.1007/s10641-018-0781-8

Brigden, K.E., Marshall, C.T., Scott, B.E., Young, E.F., and Brickle, P., 2017. Interannual variability in reproductive traits of the Patagonian toothfish *Dissostichus eleginoides* around the sub-Antarctic island of South Georgia. Journal of Fish Biology 91 (1), 278-301. doi: 10.1111/jfb.13344

Brigden, K. 2019. The reproductive ecology of Patagonian toothfish (*Dissostichus eleginoides*, Smitt 1898) around the sub-Antarctic island of South Georgia: spatial and temporal patterns and processes spanning two decades of data. PhD thesis. University of Aberdeen, UK.

Campana, S.E., Stefánsdóttir, R.B., Jakobsdóttir, K., et al., Shifting fish distributions in warming sub-Arctic oceans. Sci Rep 10, 16448 (2020). https://doi.org/10.1038/s41598-020-73444-y

Casal2 Development Team 2024. Casal2 user manual for age-based models, v24.07 (2024-07-14). National Institute of Waer & Atmospheric Research Ltd. NIWA Technical Report 139. 309p. (Using source code from https://github.com.alistairdunn/CASAL2:Development)

Cavanagh, R.D., Trathan, P.N., Hill, S.L., Melbourne-Thomas, J., Meredith, M.P., Hollyman, P., Krafft, B.A., MC Muelbert, M., Murphy, E.J., Sommerkorn, M., Turner, J., and Grant, S.M. 2021. Utilising IPCC assessments to support the ecosystem approach to fisheries management within a warming Southern Ocean. Marine Policy 131. https://doi.org/10.1016/j.marpol.2021.104589

Cavanagh, R., and Pardo, E. 2024. Progress with recommendations from the CCAMLR Workshop on Climate Change. CCAMLR Working Group on Fish Stock Assessment WG-FSA-2024/14.

Collins, M.A., Bailey, D.M., Ruxton, G.D., and Priede, I.G. 2005. Trends in body size across an environmental gradient: a differential response in scavenging and non-scavenging demersal deep-sea fish. Proceedings of the Royal Society B 272, 2051-2057.

Collins, M.A., Ross, K., Belchier, M., and Reid, K., 2007. Distribution and diet of juvenile Patagonian toothfish on the South Georgia and Shag Rocks shelves (Southern Ocean). Marine Biology 152, 135-147. https://doi.org/10.1098/rspb.2005.3189

Collins, M.A., Shreeve, R.S., Fielding, S., and Thurston, M.H., 2008. Distribution, growth, diet and foraging behaviour of the yellow-fin notothen *Patagonotothen guntheri* (Norman) on the Shag Rocks shelf (Southern Ocean). Journal of Fish Biology, 72(1), pp.271-286. https://doi.org/10.1111/j.1095-8649.2007.01711.x

Collins, M.A., Brickle, P., Brown, J., and Belchier, M. 2010. The Patagonian toothfish: biology, ecology and fishery. Advances in Marine Biology, 58, 227-300. https://doi.org/10.1016/B978-0-12-381015-1.00004-6

Combes, V., Matano, R.P., Meredith, M.P., and Young, E.F. 2023. Variability of the shelf circulation around South Georgia, Southern Ocean. Journal of Geophysical Research: Oceans, 128 (2). 13 pp. 10.1029/2022JC019257

Constable, A.J., de la Mare, W.K., Agnew, D.J., Everson, I., and Miller, D. 2000. Managing fisheries to conserve the Antarctic marine ecosystem: practical implementation of the Convention on the Conservation of Antarctic Marine Living Resources (CCAMLR). ICES Journal of Marine Science 57, 778–791. https://doi.org/10.1006/jmsc.2000.0725

Dong., S., Sprintall, J., Gille, S.T., and Talley, L. 2008. Southern Ocean mixed-layer depth from Argo float profiles. Journal of Geophysical Research: Oceans, 113(C6). https://doi.org/10.1029/2006JC004051

Donlon, C.J., Martin, M., Stark, J., Roberts-Jones, J., Fiedler, E., and Wimmer, W. 2012. The Operational Sea Surface Temperature and Sea Ice Analysis (OSTIA) system. Remote Sensing of the Environment. doi: 10.1016/j.rse.2010.10.017 2011.

Dormann, C.F., Calabrese, J.M., Guillera-Arroita, G., Matechou, E., Bahn, V., Bartoń, K., Beale, C.M., Ciuti, S., Elith, J., Gerstner, K., and Guelat, J. 2018. Model averaging in ecology: A review of Bayesian, information-theoretic, and tactical approaches for predictive inference. Ecological monographs, 88(4), pp.485-504. https://doi.org/10.1002/ecm.1309

Dunn, A. Approaches to forecasting recruitment in age-structured stock assessment modelling. CCAMLR Working Group on Statistics, Assessments and Modelling WG-SAM-2025/10

Earl, T., Readdy, L., and Marsh, J. 2023. Stock Annex for the 2023 assessment of Subarea 48.3 (South Georgia) Patagonian toothfish (*Dissostichus eleginoides*). CCAMLR Working Group on Fish Stock Assessment Paper WG-FSA-2023/56.

Earl, T., and Readdy, L. 2024. Assessment of Patagonian toothfish *(Dissostichus eleginoides*) in Subarea 48.3. CCAMLR Working Group on Fish Stock Assessment Paper WG-FSA-IMAF-2024/29.

Earl, T., Readdy, L., Alewijnse, S., Devine, J., Dunn, A., Le Clech, R., Maschette, D., Masere, C., Massiot-Granier, F., Ouzoulias, F., Péron, C. Walker, N. and Ziegler, P. 2024. Approaches to projecting recruitment in toothfish assessment models. CCAMLR Working Group on Statistics, Assessments and Modelling WG-SAM-2024/23.

Eastman, J.T. 1990. The biology and physiological ecology of notothenioid fishes. In: O. Gon, P.C. Heemstra (Eds.), Fishes of the Southern Ocean, J.L.B. Smith Institute of Ichthyology, Grahamstown (1990), pp. 34-51

Everson, I., and Murray, A., 1999. Size at sexual maturity of Patagonian toothfish. CCAMLR Sci, 6, pp.37-46.

Evseenko, S.A., Kock, K-H., Nevinsky, M.M. 1995. Early life history of the Patagonian toothfish, *Dissostichus eleginoides* Smitt, 1898 in the Atlantic sector of the Southern Ocean. Antarctic Science, 7, 221-226.

Frainer, A., Primicerio, R., Kortsch, S., Aune, M., Dolgov, A.V., Fossheim, M., Aschan, M.M. 2017. Climate-driven changes in functional biogeography of Arctic marine fish communities. Proc Natl Acad Sci USA, 114(46), 12202-12207. doi: 10.1073/pnas.1706080114.

Freer, J.J., Tarling, G.A., Collins, M., Partridge, J.C., and Genner, M.J. 2019. Predicting future distributions of lanternfish, a significant ecological resource within the Southern Ocean. Diversity and Distributions, 25. 1259-1272. 10.1111/ddi.12934

Good, S., Fiedler, E., Mao, C., Martin, M.J., Maycock, A., Reid, R., Roberts-Jones, J., Searle, T., Waters, J., While, J. and Worsfold, M., 2020. The Current Configuration of the OSTIA System for Operational Production of Foundation Sea Surface Temperature and Ice Concentration Analyses. Remote Sensing, 12 (720). doi: 10.3390/rs12040720

Gregory, S., Collins, M.A., and Belchier, M., 2017. Demersal fish communities of the shelf and slope of South Georgia and Shag Rocks (Southern Ocean). Polar Biology, 40(1), pp.107-121.

Gross, J.M., and Hoenig, J.M. Resurrecting failed environment-recruitment relationships: Revisiting cod recruitment in light of the poor-recruitment paradigm. Reviews in Fish Biology and Fisheries 35, 317–343 (2025). https://doi.org/10.1007/s11160-024-09904-9

Hefley, T.J., Broms, K.M., Brost, B.M., Buderman, F.E., Kay, S.L., Scharf, H.R., Tipton, J.R., Williams, P.J., and Hooten, M.B. 2017. The basis function approach for modeling autocorrelation in ecological data. Ecology, 98(3), pp.632-646. https://doi.org/10.1002/ecy.1674

Hogg, O.T., Cavanagh, R.D, Grant, S., Belchier, M., Gregory, S., and Collins, M.A., 2021. Key climate change effects on the coastal and marine environment around the Polar UK Overseas Territories. Marine Climate Change Impacts Partnership Science Review. 0.14465/2021.orc02.pol

Hollyman, P.R., Hill, S.L., Laptikhovsky, V.V., Belchier, M., Gregory, S., Clement, A., Collins, M.A. 2021. A long road to recovery: dynamics and ecology of the marbled rockcod (*Notothenia rossii*, family: Nototheniidae) at South Georgia, 50 years after overexploitation. ICES Journal of Marine Science, 78(8): 2745-2756. https://doi.org/10.1093/icesjms/fsab150

Hollyman, P.R., Soeffker, M., Roberts, J., Hogg, O.T., Laptikhovsky, V.V., Queirós, J.P., Darby, C., Belchier, M., Collins, M.A. 2022. Bioregionalization of the South Sandwich Islands through community analysis of bathyal fish and invertebrate assemblages using fishery-derived data. Deep Sea Research Part II: Topical Studies in Oceanography, 198 (). 15 pp. 10.1016/j.dsr2.2022.105054

Hollyman, P.R., Hill, S.L., Gunn, C., Keith, P. Rodriguez, B. and Collins M.A. 2023. Report of the UK Groundfish Survey at South Georgia (CCAMLR Subarea 48.3) in February 2023. CCAMLR Working Group on Fish Stock Assessment Paper WG-FSA-2023/45 Rev 1.

Howard, R., Rogers, L., Kearney, K., Vary, L., and Ciannelli, L. 2024. Projecting marine fish distributions during early life stages under future climate scenarios. Fish and Fisheries. DOI 10.1111/faf.12835

Huserbråten, M.B.O., Eriksen, E., Gjøsæter, H., et al. 2019. Polar cod in jeopardy under the retreating Arctic sea ice. Commun Biol 2, 407. https://doi.org/10.1038/s42003-019-0649-2

IPCC 2019. IPCC Special Report on the Ocean and Cryosphere in a Changing Climate [Portner, H.-O., Roberts, D.C., Masson-Delmotte, V., Zhai, P., Tignor, M., Poloczanska, E. et al., (eds.)], 2019. https://www.ipcc.ch/srocc/

IPCC 2022. Climate Change 2022: Impacts, Adaptation and Vulnerability. Contribution of Working Group II to the Sixth Assessment Report of the Intergovernmental Panel on Climate Change (Eds. H.-O. Pörtner, et al.,) (IPCC, Geneva, 2022).

Jones, T., Cavanagh, R.D., Thorpe, S.E., Earl, T., Freer, J.J., Hill, S.L., Waluda, C.M., and Collins, M.A. 2025. Spatial and environmental factors associated with Patagonian toothfish (*Dissostichus eleginoides*) distribution at South Georgia and the South Sandwich Islands. CCAMLR WG-FSA-2025/XX

Laurel, B.J., Copeman, L.A., Spencer, M. and Iseri, P. 2018 Comparative effects of temperature on rates of development and survival of eggs and yolk-sac larvae of Arctic cod (*Boreogadus saida*) and walleye pollock (*Gadus chalcogrammus*) ICES Journal of Marine Science, Volume 75, Issue 7, December 2018, Pages 2403–2412, https://doi.org/10.1093/icesjms/fsy042

Lellouche, J. M., Greiner, E., Bourdalle-Badie, R., Garric, G., Melet, A., Drevillon, M., et al. (2021). The Copernicus Global 1/12° Oceanic and Sea Ice GLORYS12 Reanalysis. Frontiers in Earth Science, 9, Article ID: 698876. https://doi.org/10.3389/feart.2021.698876

Levine, R., Robertis, A., Grunbaum, D., Wildes, S., Farley, E., Stabeno, P., and Wilson, C. 2023. Climate-driven shifts in pelagic fish distributions in a rapidly changing Pacific Arctic. Deep Sea Research Part II: Topical Studies in Oceanography. 208. 105244. 10.1016/j.dsr2.2022.105244

Ljungström, G., Langbehn, T.J. and Jørgensen, C. Light and energetics at seasonal extremes limit poleward range shifts. Nat. Clim. Chang. 11, 530–536 (2021). https://doi.org/10.1038/s41558-021-01045-2

Kammann, E.E. and Wand, M.P. 2003. Geoadditive models. Journal of the Royal Statistical Society Series C: Applied Statistics, 52(1), pp.1-18.

Meredith, M.P., Brandon, M.A., Murphy, E.J., Trathan, P.N., Thorpe, S.E., Bone, D.G., Chernyshkov, P. P., and Sushin, V.A. 2005. Variability in hydrographic conditions to the east and northwest of South Georgia, 1996–2001. Journal of Marine Systems, 53 (1-4): 143-167. doi:10.1016/j.jmarsys.2004.05.005

Murphy, E.J., Trathan, P.N., Watkins, J.L., Reid, K., Meredith, M.P., Forcada, J., Thorpe, S.E., Johnston, N.M., and Rothery, P. 2007. Climatically driven fluctuations in Southern Ocean ecosystems. Proceedings of the Royal Society B: Biological Sciences, 274 (). pp. doi:10.1098/rspb.2007.1180

NOAA National Centers for Environmental Information. 2022. ETOPO 2022 15 Arc-Second Global Relief Model. NOAA National Centers for Environmental Information. https://doi.org/10.25921/fd45-gt74 . Accessed 3-March-2024.

North, A.W. 2002. Larval and juvenile distribution and growth of Patagonian toothfish around South Georgia. Antarctic Science 14, Issue 1. doi.org/10.1017/S0954102002000548

Ouzoulias, F., Massiot-Granier, F., Alewijnse, S., Devine, J., Dunn, A., Earl, T., Le Clech, R., Maschette, D., Masere, C., Péron, C., Readdy, L., Walker, N. and Ziegler, P. 2024. Effects of implementing dynamic B0 in toothfish fisheries. CCAMLR Working Group on Statistics, Assessments and Modelling WG-SAM-2024/25.

Park Y.-H., Park T., Kim T.-W., Lee S.-H., Hong C.-S., Lee J.-H., Rio M.-H., Pujol M.-I., Ballarotta M., Durand I., and Provost C. 2019. Observations of the Antarctic Circumpolar Current over the Udintsev Fracture Zone, the narrowest choke point in the Southern Ocean. Journal of Geophysical Research: Oceans, 124 (7): 4511-4528. https://doi.org/10.1029/2019JC015024

Park, Y.-H, and Durand, I. 2019. Altimetry-derived Antarctic Circumpolar Current fronts. SEANOE. https://doi.org/10.17882/59800

Pinheiro, J., Bates, D.R. Core Team (2025). nlme: Linear and Nonlinear Mixed Effects Models. R package version 3.1-167, <https://CRAN.R-project.org/package=nlme>.

R Core Team (2024). R: A Language and Environment for Statistical Computing. R Foundation for Statistical Computing, Vienna, Austria. <https://www.R-project.org/>.

Rogers, A.D., Morley, S., Fitzcharles, E., Jarvis, K., and Belchier, M. 2006. Genetic structure of Patagonian toothfish (*Dissostichus eleginoides*) populations on the Patagonian shelf and Atlantic and western Indian ocean sectors of the Southern Ocean. Mar. Biol. 149, 915–924. https://doi.org/10.1007/s00227-006-0256-x

Saunders, R.A., Hollyman, P.R., Thorpe, S.E., and Collins, M.A. 2022. Population characteristics of benthopelagic *Gymnoscopelus nicholsi* (Pisces: Myctophidae) on the continental shelf of South Georgia (Southern Ocean) during austral summer. Polar Biology, 45:789-807 10.1007/s00300-022-03033-4

SC-CAMLR-42. 2023. Report of the Forty-Second Meeting of the Scientific Committee, Hobart, Australia 16 – 20 October 2023. https://meetings.ccamlr.org/system/files/meeting-reports/e-sc-42-rep.pdf

Shaw, P.W., Arkhipkin, A.I., and Al-Khairulla, H. 2004. Genetic structuring of Patagonian toothfish populations in the Southwest Atlantic Ocean: the effect of the Antarctic Polar Front and deep-water troughs as barriers to genetic exchange. Molecular Ecology 13 (11), 3293–3303. https://doi.org/10.1111/j.1365-294x.2004.02327.x

Soeffker, M., Hollyman, P.R., Collins, M.A., Hogg, O.T., Riley, A., Laptikhovsky, V., Earl, T., Roberts, J., MacLeod, E., Belchier, M., and Darby, C. 2022. Contrasting life-history traits of two toothfish (Dissostichus spp.) species at their range edge around the South Sandwich Islands. Deep Sea Research Part II: Topical Studies in Oceanography 201, 105098. doi: 10.1016/j.dsr2.2022.105098

Thorpe, S.E., and Murphy, E.J. 2022. Spatial and temporal variability and connectivity of the marine environment of the South Sandwich Islands, Southern Ocean. Deep Sea Research Part II: Topical Studies in Oceanography, 198 105057. 16 pp. 10.1016/j.dsr2.2022.105057

Tsoukali, S., Visser, A.W., and MacKenzie, B.R. 2016. Functional responses of North Atlantic fish eggs to increasing temperature. Marine Ecology Progress Series 555:151-165 https://doi.org/10.3354/meps11758

Ward, D., Hill, N., Melbourne-Thomas, J., Welsford, D., Arangio, R., McNeill, M., Wotherspoon, S., Ziegler, P., and Corney, S. 2025. Exploring mechanisms of change in a Southern Ocean fishery with a co-produced network model. ICES Journal of Marine Science. 82. 10.1093/icesjms/fsaf095.

Welsford, D. 2023. Summary and Recommendations from Independent review of CCAMLR toothfish assessments, 2023. SC-CAMLR-42/02 Rev. 2

Whitehouse, M.J., Meredith, M.P., Rothery, P., Atkinson, A., Ward, P., and Korb, R.E. (2008) Rapid warming of the ocean around South Georgia, Southern Ocean, during the 20th century: Forcings,

characteristics and implications for lower trophic levels. Deep-Sea Research Part I, 55 (10), 1218-1228. doi:10.1016/j.dsr.2008.06.002

WG-FSA-IMAF-2024. Report of the Working Group on Fish Stock Assessment and Incidental Mortality Associated with Fishing. Hobart, Australia, 30 September to 11 October 2024. https://meetings.ccamlr.org/en/sc-camlr-43/14

Wood, S.N. 2011. Fast stable restricted maximum likelihood and marginal likelihood estimation of semiparametric generalized linear models. Journal of the Royal Statistical Society (B) 73(1):3-36. https://doi.org/10.1111/j.1467-9868.2010.00749.x

Zhivov, V.V., and Krivoruchko V.M. 1990. On the biology of the Patagonian toothfish, *Dissostichus eleginoides*, of the Antarctic part of the Atlantic. Journal of lchthyology 30(7): 142-146.

Supplementary materials

Section 1: Additional information on groundfish survey data

Table S1. *Summary of bottom-trawl surveys used in analyses of Patagonian toothfish (Dissostichus eleginoides) distribution. All values presented are after data-cleaning and represent sample sizes entering analyses. Design abbreviations: SRS = stratified random sample, RAD = radial, DW = deepwater trawl surveys.*

Survey	Date start	Date end	Gear	Design	Trawls
SG87	29-Nov-86	17-Dec-86	B-454 OT	SRS	104
SG88	19-Dec-87	12-Jan-88	P32/36 OT	SRS	112
SG89	1-Feb-89	14-Feb-89	P32/36 OT	SRS	55
SG90	6-Jan-90	26-Jan-90	HC120 OT	SRS	68
SG91	22-Jan-91	11-Feb-91	FP120	SRS	77
SG92	3-Jan-92	26-Jan-92	FP120	SRS	81
SG94	4-Jan-94	8-Feb-94	FP120	SRS	81
SG97	2-Sep-97	29-Sep-97	FP120	SRS	55
SG00	16-Jan-00	30-Jan-00	FP120	SRS	41
SG02	12-Jan-02	1-Feb-02	FP120	SRS	63
SG03	7-Jan-03	31-Jan-03	FP120	RAD	38
SG04	7-Jan-04	5-Feb-04	FP120	SRS	64
SG05	7-Jan-05	25-Jan-05	FP120	SRS	42
SG06	3-Jan-06	1-Feb-06	FP120	SRS	66
SG07	27-Aug-07	21-Sep-07	FP120	SRS	49
SG08	16-Apr-08	30-Apr-08	FP120	SRS	70
SG09	15-Jan-09	23-Jan-09	FP120	SRS	73
SG10	15-Jan-10	24-Jan-10	FP120	SRS	75
DW10	29-Jan-10	31-Jan-10	FP120	DW	6
SG11	26-Jan-11	6-Feb-11	FP120	SRS	87
SG12	26-Jan-12	29-Jan-12	FP120	SRS[a]	22
SG13	22-Jan-13	29-Jan-13	FP120	SRS	68
SG15	13-Jan-15	23-Jan-15	FP120	SRS	77
SG17	30-Jan-17	7-Feb-17	FP120	SRS	72
DW19	5-Feb-19	5-Feb-19	FP120	DW	3
SG19	27-Jan-19	5-Feb-19	FP120	SRS	73
SG21	8-May-21	28-May-21	FP120	SRS	76
SG23	1-Feb-23	10-Feb-23	FP120	SRS	75

a: 2012 survey was incomplete, with sampling only on Shag Rocks and the NW South Georgia shelf

Section 2: Results of analyses of juvenile toothfish abundance at Shag Rocks

Inclusion of spatial effects in analyses of juvenile abundance

Gaussian process smooths included to model spatial effects in our analyses of juvenile abundance were specified using a Matern correlation function with spatial range parameter, r, which we varied from 10 – 100 km in 10 km jumps to control the degree of spatial smoothing/continuity. We also tested stationary (no continuous trend in space) versus non-stationary (a continuous trend in a given direction) spatial effects. Both range and stationarity of spatial fields were altered by modifying the m argument in the Gaussian process smooth. We then selected among models with alternate range parameters based on minimising AIC to identify our null model for subsequent testing (**Table S2**). For $Sz_{<26}$ fish a stationary spatial field with range = 40 km resulted in the lowest AIC, whereas models containing spatial effects for $Sz_{26\text{-}37}$ fish performed no better than the model containing depth alone.

Table S2. *Comparison between alternate null models for examining interannual variability in abundance of < 26 cm and 26-37 cm size-classes of Patagonian toothfish at Shag Rocks. The range parameter controlling the degree of spatial smoothing is given in () when spatial terms (Space) were included. Values correspond to the estimated model degrees of freedom (edf), deviance explained (D^2) and Akaike's Information Criterion (AIC). Results are only presented for stationary spatial effects as these outperformed the non-stationary alternative for both age-classes. The model with lowest AIC for each age-class is highlighted in* ***bold****.*

	L: < 26 cm			L: 26-37 cm		
Model	**df**	**D^2**	**AIC**	**df**	**D^2**	**AIC**
Survey	16.8	58.4	359.8	18.9	54.0	1043.8
Survey + Depth	20.1	78.0	319.9	**23.1**	**58.9**	**1029.7**
Survey + Depth + Space (10 km)	24.7	80.5	320.1	29.3	60.2	1035.7
Survey + Depth + Space (20 km)	23.3	80.3	317.9	23.1	58.9	1029.8
Survey + Depth + Space (30 km)	22.5	80.1	317.1	23.1	58.9	1029.8
Survey + Depth + Space (40 km)	22.1	79.9	316.8	23.1	58.9	1029.8
Survey + Depth + Space (50 km)	**21.9**	**79.8**	**316.8**	23.1	58.9	1029.8
Survey + Depth + Space (60 km)	21.8	79.8	316.8	23.1	58.9	1029.8
Survey + Depth + Space (70 km)	21.7	79.7	316.9	23.1	58.9	1029.8
Survey + Depth + Space (80 km)	21.6	79.6	317.0	23.1	58.9	1029.8
Survey + Depth + Space (90 km)	21.5	79.6	317.1	23.1	58.9	1029.8
Survey + Depth + Space (100 km)	21.5	79.5	317.1	23.1	58.9	1029.8

Cross validation and calculation of prediction error

Models examining variation in juvenile abundance at Shag Rocks were compared based on cross-validated predictive error, where cross-validation was performed by fitting the model to data from k-1 (k=19) surveys and evaluating model predictions on counts in the held-out survey. This effectively tests the ability of temperature relationships to predict abundance in an unseen year. Predictive error was quantified using a likelihood-based score (Dormann et al. 2018), equal to the log-likelihood of the data in each held-out survey given predictions from the model trained on the remaining data:

$$\mathcal{L} = \sum_{j=1}^{k} \ell\left(y_{[j]} | \widehat{y_{[j]}}, \hat{\theta}\right)$$

Where $\mathcal{L}$ is the likelihood score, $\ell\left(y_{[j]} | \widehat{y_{[j]}}, \hat{\theta}\right)$ is the log-likelihood of counts, $y_{[j]}$ in the held-out survey *j*, given predicted values $\widehat{y_{[j]}}$ and dispersion $\hat{\theta}$ from the model fitted to the remaining data. The model fitted to the data (described in the main text) was a Generalised Additive Mixed Model (GAMM) estimated assuming that counts were distributed according to a negative-binomial distribution. As such, the log-likelihood of the held-out data given model predictions, $\ell\left(y_{[j]} | \widehat{y_{[j]}}, \hat{\theta}\right)$, was calculated according to the sum of log probability densities evaluated for a negative-binomial probability distribution evaluated at $y_{[j]}$ with mean $\widehat{y_{[j]}}$ and dispersion $\hat{\theta}$. For interpretability, likelihood scores were converted to a measure akin to deviance explained by calculating the ratio of the difference in likelihood score between the focal model, $\mathcal{L}_{mod}$, and the null model, $\mathcal{L}_{null}$, relative to the difference in likelihood score between the null model and the best possible model, $\mathcal{L}_{best}$:

$$D_{mod} = \frac{\mathcal{L}_{null} - \mathcal{L}_{mod}}{\mathcal{L}_{null} - \mathcal{L}_{best}}$$

The likelihood score for the null model was calculated through cross-validation as described above, and because the null model represented interannual variability only via random effects, it effectively explains none of the interannual variability in a predictive sense (i.e., the prediction for a held-out survey is the average, or intercept after controlling for depth and spatial variability, of the years

included in the training dataset). The likelihood score for the best possible model was taken to be the log-likelihood of a model where all interannual variability (but not all variability, i.e. not a fully saturated model) is explained via the inclusion of a fixed survey effect. The resulting measure, D_{mod}, ranges from 0 to 1 and represents the improvement in log-likelihood of model predictions compared to a model where no interannual variability is explained, relative to the best possible scenario where model predictions for held-out surveys match those where all interannual variability is explained.

Table S3. *Statistics for models examining interannual variability in abundance of < 26 cm Patagonian toothfish at Shag Rocks according to temperature in different seasons (Spawn = Jun-Aug, Egg = Sep-Nov, Larvae = Dec-Feb, Settlement = Mar-May), locations (SR = Shag Rocks, SG = South Georgia), and depth strata. Statistics include AIC, the predictive likelihood (pLik) score calculated via survey-stratified cross-validation, which is also used to calculate a measure of predictive deviance (pD) by comparison to the likelihood of a model where all interannual variability is explained via a fixed survey effect (Likelihood = 133.15). Models that improve on the null model based on predictive cross-validation scores are highlighted in* ***red****.*

			Mod: NULL + s(Temp)			Mod: NULL + s(Temp) + s(Date)		
Stage	**Area**	**Depth (range, m)**	**AIC**	**pLik**	**pD**	**AIC**	**pLik**	**pD**
NULL			316.8	321.6	0.00	316.6	277.0	0.24
Spawn	SR	Midwater (110-267 m)	316.6	330.5	-0.05	316.7	371.4	-0.26
Spawn	SR	Midwater (267-454 m)	316.7	321.6	0.00	316.7	290.6	0.16
Spawn	SR	Seafloor (< 267 m)	316.8	331.2	-0.05	317.0	282.3	0.21
Spawn	SR	Seafloor (644-1063 m)	316.7	344.0	-0.12	317.7	277.6	0.23
Spawn	SG	Midwater (110-267 m)	316.8	343.5	-0.12	316.8	283.1	0.20
Spawn	SG	Midwater (267-454 m)	316.7	358.9	-0.20	316.5	300.1	0.11
Spawn	SG	Seafloor (< 267 m)	317.0	322.7	-0.01	**316.8**	**268.5**	**0.28**
Spawn	SG	Seafloor (644-1063 m)	317.2	350.4	-0.15	317.2	294.9	0.14
Egg	SR	Surface	317.8	532.4	-1.12	317.8	392.4	-0.38
Egg	SR	Midwater (110-267 m)	**315.8**	**192.4**	**0.69**	**317.5**	**202.6**	**0.63**
Egg	SR	Midwater (267-454 m)	316.6	340.9	-0.10	316.5	289.8	0.17
Egg	SG	Surface	318.5	369.9	-0.26	318.6	354.3	-0.17
Egg	SG	Midwater (110-267 m)	**317.0**	**302.3**	**0.10**	316.9	303.8	0.09
Egg	SG	Midwater (267-454 m)	316.3	368.6	-0.25	316.1	326.8	-0.03
Larvae	SR	Surface	**318.3**	**299.2**	**0.12**	**317.8**	**231.0**	**0.48**
Larvae	SR	Midwater (110-267 m)	**318.9**	**199.9**	**0.65**	**320.0**	**212.9**	**0.58**
Larvae	SR	Midwater (267-454 m)	316.2	339.5	-0.09	317.4	396.5	-0.40
Larvae	SG	Surface	**317.6**	**270.2**	**0.27**	**316.9**	**233.6**	**0.47**
Larvae	SG	Midwater (110-267 m)	**315.2**	**212.5**	**0.58**	**316.7**	**201.5**	**0.64**
Larvae	SG	Midwater (267-454 m)	317.9	382.5	-0.32	316.5	326.7	-0.03
Settlement	SR	Surface	315.4	370.4	-0.26	314.9	307.4	0.08
Settlement	SR	Seafloor (< 267 m)	**319.2**	**251.8**	**0.37**	317.6	291.1	0.16

Table S4. *Statistics for models examining interannual variability in abundance of 26-37 cm Patagonian toothfish at Shag Rocks according to temperature in different seasons (Spawn = Jun-Aug, Egg = Sep-Nov, Larvae = Dec-Feb, Settlement = Mar-May), locations (SR = Shag Rocks, SG = South Georgia), and depth strata. Statistics include AIC, the predictive likelihood (pLik) score calculated via survey-stratified cross-validation, which is also used to calculate a measure of predictive deviance (pD) by comparison to the likelihood of a model where all interannual variability is explained via a fixed survey effect (Likelihood = 489.6). Models that improve on the null model based on predictive cross-validation scores are highlighted in* ***red****.*

			Mod: NULL + s(Temp)			Mod: NULL + s(Temp) + s(Date)		
Stage	**Area**	**Depth**	**AIC**	**pLik**	**pD**	**AIC**	**pLik**	**pD**
NULL			1029.7	944.8	0.00	1030.2	953.6	-0.02
Spawn	SR	Midwater (110-267 m)	**1028.3**	**739.5**	**0.45**	**1028.1**	**800.8**	**0.31**
Spawn	SR	Midwater (267-454 m)	1029.4	1023.8	-0.17	1029.8	1074.5	-0.28
Spawn	SR	Seafloor (< 267 m)	**1027.8**	**631.8**	**0.69**	**1028.0**	**649.6**	**0.64**
Spawn	SR	Seafloor (644-1063 m)	**1029.5**	**940.0**	**0.01**	**1029.6**	**921.6**	**0.05**
Spawn	SG	Midwater (110-267 m)	**1028.7**	**863.5**	**0.18**	1029.0	1027.8	-0.18
Spawn	SG	Midwater (267-454 m)	1029.4	1081.3	-0.30	1029.8	1310.2	-0.79
Spawn	SG	Seafloor (< 267 m)	1029.3	1349.5	-0.89	1029.6	2000.0	-2.27
Spawn	SG	Seafloor (644-1063 m)	1029.6	968.0	-0.05	**1029.7**	**885.2**	**0.13**
Egg	SR	Surface	1029.7	1001.3	-0.12	1029.7	952.5	-0.02
Egg	SR	Midwater (110-267 m)	**1029.6**	**865.9**	**0.17**	**1028.5**	**905.3**	**0.09**
Egg	SR	Midwater (267-454 m)	1029.0	1134.9	-0.42	1029.6	1382.2	-0.94
Egg	SG	Surface	1029.7	996.4	-0.11	1029.7	1124.5	-0.39
Egg	SG	Midwater (110-267 m)	**1028.8**	**848.4**	**0.21**	1028.8	960.7	-0.03
Egg	SG	Midwater (267-454 m)	1029.4	1838.3	-1.96	1028.9	2695.6	-3.77
Larvae	SR	Surface	1029.7	1088.0	-0.31	1030.3	991.8	-0.10
Larvae	SR	Midwater (110-267 m)	1030.4	1020.3	-0.17	1030.4	1153.0	-0.45
Larvae	SR	Midwater (267-454 m)	1029.8	1276.2	-0.73	1030.0	1194.8	-0.54
Larvae	SG	Surface	1029.6	1010.2	-0.14	1029.8	1052.8	-0.23
Larvae	SG	Midwater (110-267 m)	**1029.6**	**873.4**	**0.16**	1029.7	1000.5	-0.12
Larvae	SG	Midwater (267-454 m)	1029.6	1083.6	-0.30	1030.2	2700.1	-3.78
Settlement	SR	Surface	1029.7	1655.8	-1.56	1029.2	1352.4	-0.88
Settlement	SR	Seafloor (< 267 m)	1027.8	1005.5	-0.13	1028.0	970.9	-0.06

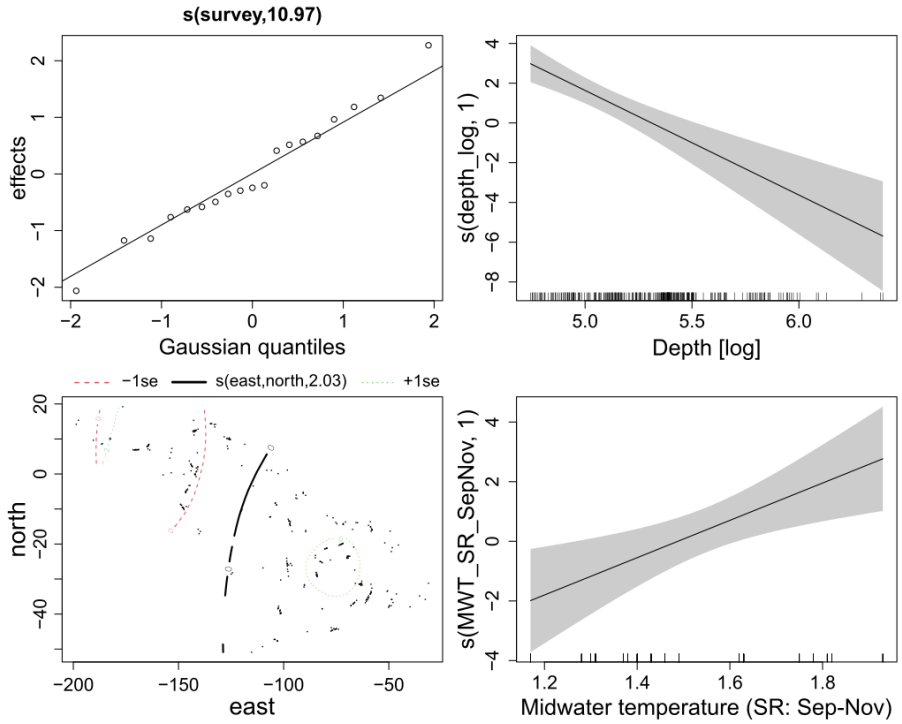

Figure S1. *Fitted effects from the best-predicting model for abundance of the < 26 cm size-class of Patagonian toothfish at Shag Rocks. Panels correspond to survey random effects, and fitted smooths for (log-transformed) depth (thin-plate regression spline, basis='tp'), easting and northing (Gaussian process, basis='gp'), and midwater temperature during egg-dispersal (September-November) at Shag Rocks (thin-plate regression spline, basis='tp'). Smooth effects show the mean with shading corresponding to 2 standard errors.*

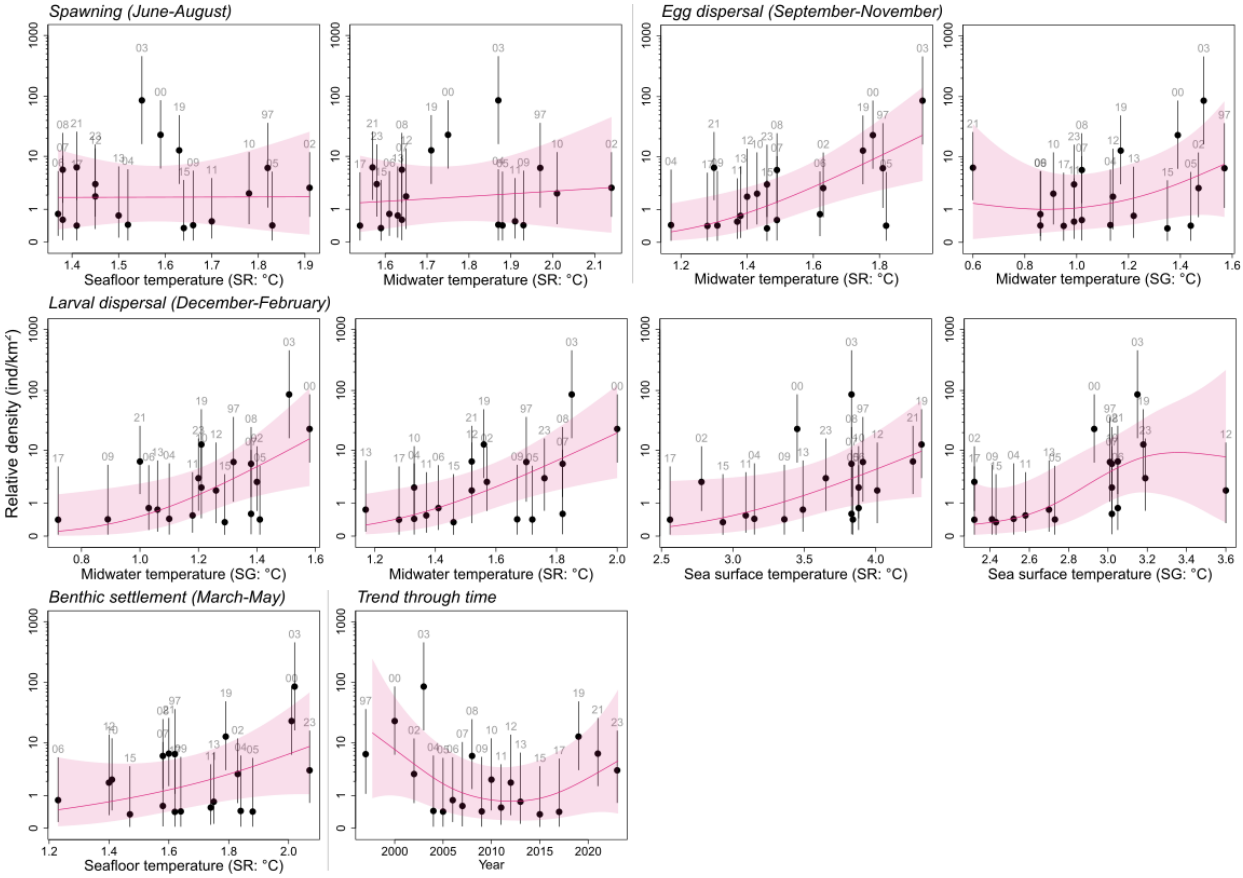

Figure S2. *Relationships between temperature and survey-average abundance of < 26 cm Patagonian toothfish at Shag Rocks. Panels correspond to fitted relationships for each temperature metric, which were created based on combinations of time-periods relevant to toothfish early development, position in the water column (surface, midwater, seafloor) and shelf area (SR = Shag Rocks, SG = South Georgia). Midwater temperatures were those calculated at 110-267 m depth, and seafloor temperatures were calculated for locations shallower than 267 m. Fitted trends through time are also shown. Survey-average abundance is shown as the mean, with error bars indicating ± 2 SE, and fitted relationships (red) indicate the mean with shading indicating ± 2 SE.*

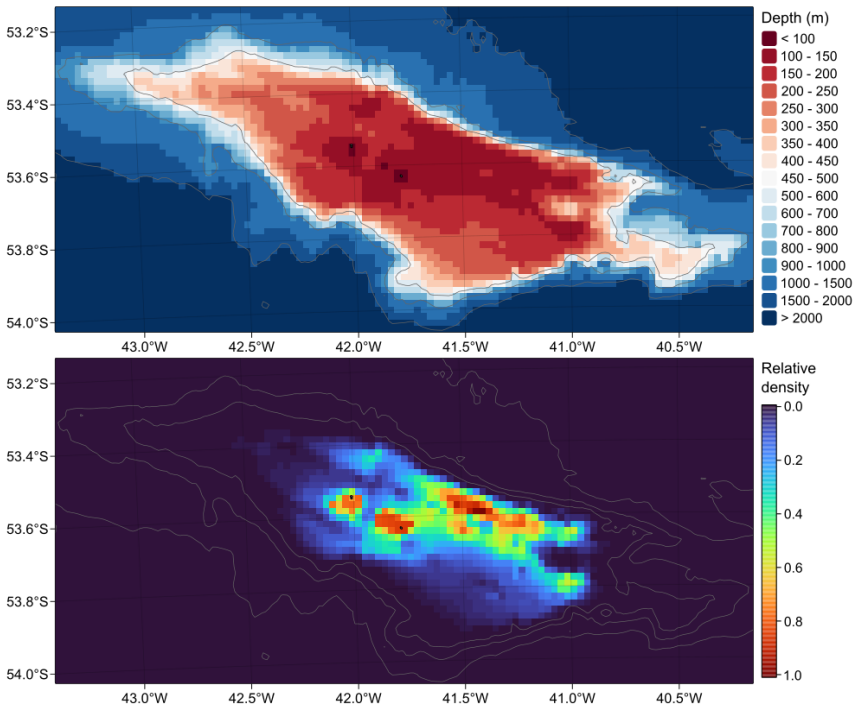

Figure S3. *Estimated relative distribution of the < 26 cm size-class of Patagonian toothfish at Shag Rocks in relation to bathymetry. Panels correspond to the bathymetry of the Shag Rocks shelf (upper), and the projected distribution from the best-predicting model fitted to counts of < 26 cm toothfish (lower) according to fitted depth and spatial effects. Predicted distribution is relative density (predicted density/max predicted density) rather than absolute density as the model contained temporal effects which scale up/down absolute density but have no impact on distribution.*

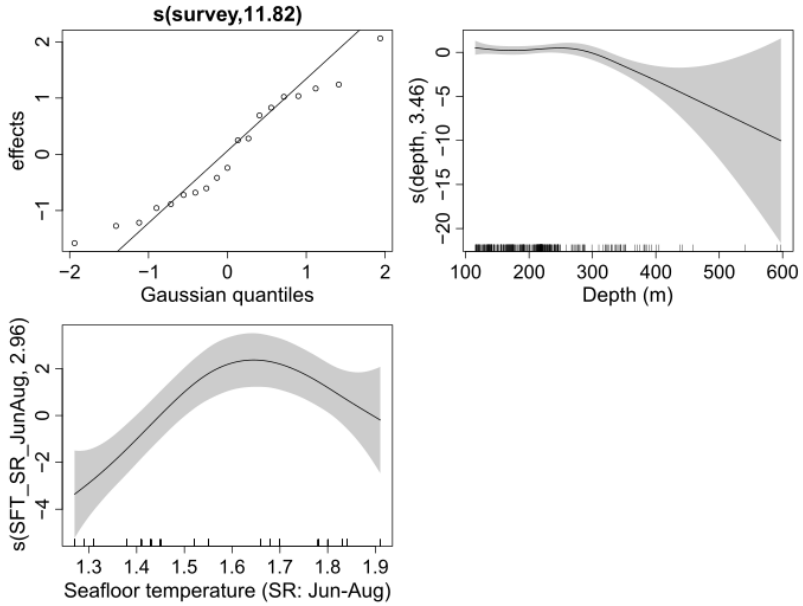

Figure S4. *Fitted effects from the best-predicting model for abundance of the 26-37 cm size-class of Patagonian toothfish at Shag Rocks. Panels correspond to survey random effects and fitted smooths for depth (thin-plate regression spline, basis='tp'), and seafloor temperature during spawning (June-August) at Shag Rocks (thin-plate regression spline, basis='tp'). Smooth effects show the mean with shading corresponding to 2 standard errors.*

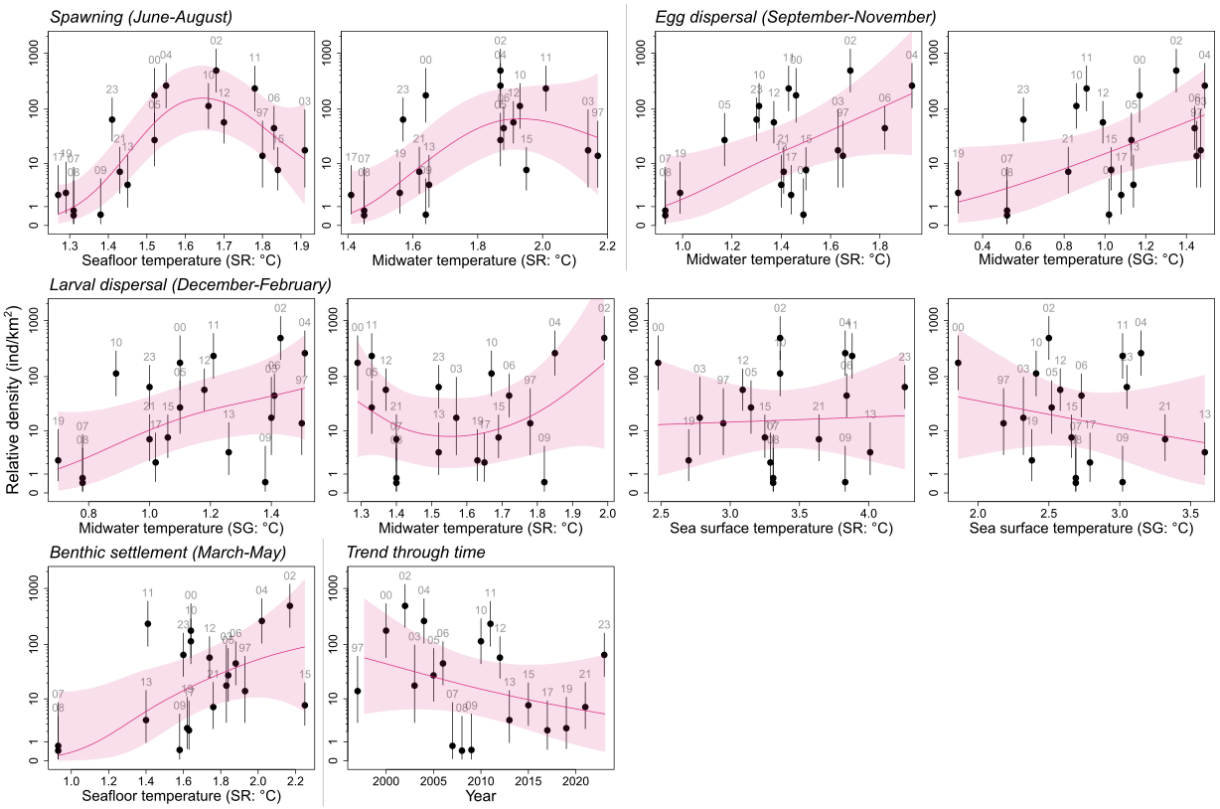

Figure S5. *Relationships between temperature and survey-average abundance of 26-37 cm Patagonian toothfish at Shag Rocks. Panels correspond to fitted relationships for each temperature metric, which were created based on combinations of time-periods relevant to toothfish early development, position in the water column (surface, midwater, seafloor) and shelf area (SR = Shag Rocks, SG = South Georgia). Midwater temperatures were those calculated at 110-267 m depth, and seafloor temperatures were calculated for locations shallower than 267 m. Fitted trends through time are also shown. Survey-average abundance is shown as the mean, with error bars indicating ± 2 SE, and fitted relationships (red) indicate the mean with shading indicating ± 2 SE.*

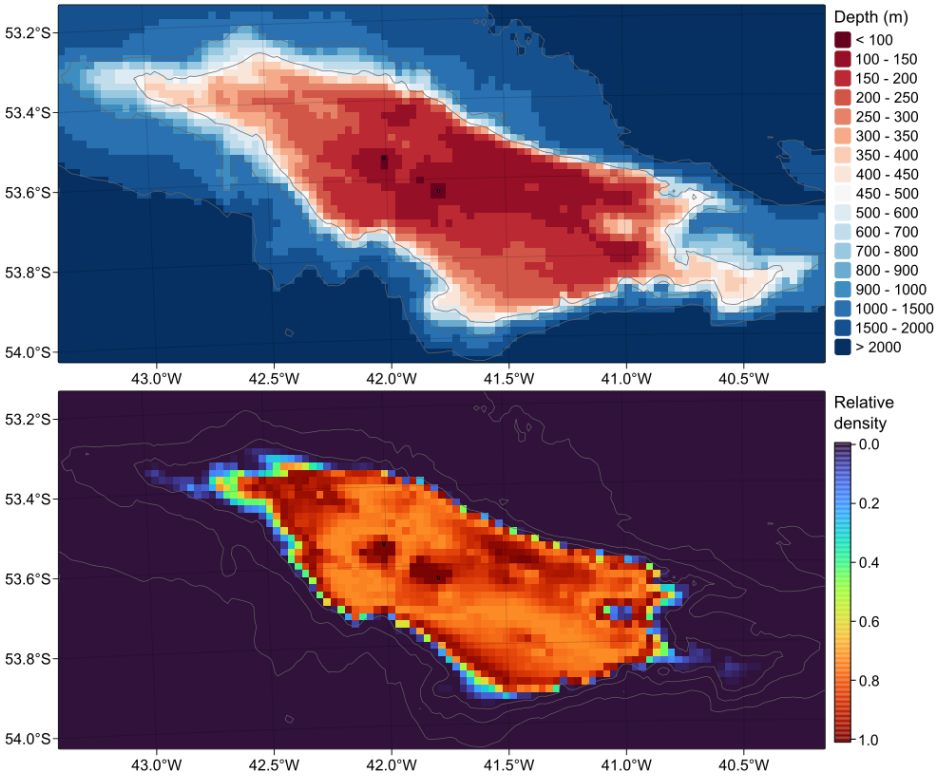

Figure S6. *Estimated relative distribution of the 26-37 cm size-class of Patagonian toothfish at Shag Rocks in relation to bathymetry. Panels correspond to the bathymetry of the Shag Rocks shelf (upper), and the projected distribution from the best-predicting model fitted to counts of 26-37 cm toothfish (lower) according to fitted depth and spatial effects. Predicted distribution is relative density (predicted density/max predicted density) rather than absolute density as the model contained temporal effects which scale up/down absolute density but have no impact on distribution.*

Section 3: Classification of year-class strength

Table S5. *Classification of year-class strength of Patagonian toothfish (Dissostichus eleginoides) according to spawning year. Year-class strength was quantified as high, average or low, according to the empirical mean CPUE (ind./km^2) of < 26 cm and 26-37 cm size-classes (assigned to spawning year by a 1.5 or 2.5 year offset, respectively), and according to survey random effects (expressed as z-scores; Model est.) from a model fitted to trawl counts, accounting for differences in trawl locations and depth among surveys. Estimates of year class strength are colour-coded based on whether they occur in the lower (red) or upper (blue) quartiles of the distribution of values among years. Where classifications of year class strength disagree between < 26 cm and 26-37 cm size-classes, the overall classification (Consensus) was based on the 26-37 cm classification.*

Spawn-	L: < 26 cm			L: 26-37 cm			
year	Survey	Mean CPUE	Model est.	Survey	Mean CPUE	Model est.	Consensus
1984				SG87	100.4	0.61	ave
1985	SG87	19.1	-0.71	SG88	171.9	0.50	ave
1986	SG88	**313.0**	0.14	SG89*			ave
1987				SG90	26.0	-0.19	ave
1988	SG90	**9157.5**	**2.10**	SG91	**554.0**	**1.33**	high
1989	SG91	**76.7**	0.04	SG92	**363.5**	**1.21**	high
1990	SG92	21.6	-0.12				ave
1991				SG94	**225.6**	**0.79**	high
1992	SG94	**818.3**	**0.88**				high
1993							
1994							
1995				SG97	7.2	-0.39	ave
1996	SG97	13.5	-0.02				ave
1997				SG00	181.4	0.76	ave
1998	SG00	**109.0**	0.55				ave
1999				SG02	**435.2**	**1.37**	high
2000	SG02	6.8	-0.40	SG03	8.3	-0.28	ave
2001	SG03	**224.9**	**1.75**	SG04	**181.7**	**1.11**	high
2002	SG04	**0.0**	**-1.33**	SG05	24.0	-0.05	ave
2003	SG05	**0.0**	**-1.33**	SG06	46.2	0.09	ave
2004	SG06	**0.8**	**-0.89**				low
2005				SG08	**0.0**	**-2.05**	low
2006	SG08	5.7	0.39	SG09	**0.0**	**-2.00**	low
2007	SG09	**0.0**	**-1.11**	SG10	121.7	0.64	ave
2008	SG10	5.8	-0.09	SG11	**266.1**	**1.03**	high
2009	SG11	**0.8**	**-1.01**	SG12	57.0	0.34	ave
2010	SG12	**0.8**	-0.53	SG13	**3.3**	**-1.06**	low
2011	SG13	1.1	-0.64				ave
2012				SG15	**7.0**	**-0.72**	low
2013	SG15	**0.0**	**-1.07**				low
2014				SG17	**1.7**	**-1.32**	low
2015	SG17	**0.0**	**-0.86**				low
2016				SG19	**2.0**	**-1.27**	low
2017	SG19	20.0	**1.51**				ave
2018				SG21	**6.4**	**-0.75**	low
2019	SG21	8.5	**1.32**				ave
2020				SG23	67.0	0.37	ave
2021	SG23	1.8	**0.81**				ave

*: While a groundfish survey was performed in 1989, no trawl data were collected from the Shag Rocks shelf

Section 4: Additional temperature results

Validation of water column temperature

Given concerns related to reliance on model-derived seawater temperature from the GLORYSv12 dataset, we obtained data collected in-situ from nine CTD deployments (**Figure S7**) at South Georgia in 2023 and compared the resultant vertical temperature profiles to equivalent profiles extracted from the GLORYSv12 dataset. For each CTD deployment, we extracted temperature data from the GLORYSv12 dataset on the date of CTD deployment from each depth layer in the grid cell nearest to the CTD location. This enabled us to construct a time- and location-matched vertical temperature profile from the GLORYSv12 dataset for each CTD deployment. In our comparisons, we compare values for each individual CTD deployment, but also compare the aggregated profiles for April, July, and September, given that CTD deployments were collected in close proximity (except for deployments in September; **Figure S7**) and over the space of 2-3 days within each month. The rationale for comparing vertical temperature profiles in aggregate is that the model informing the GLORYSv12 dataset may not be able to resolve small scale or short-term variability in temperature, but ought to perform better at explaining patterns aggregated across multiple in-situ observations.

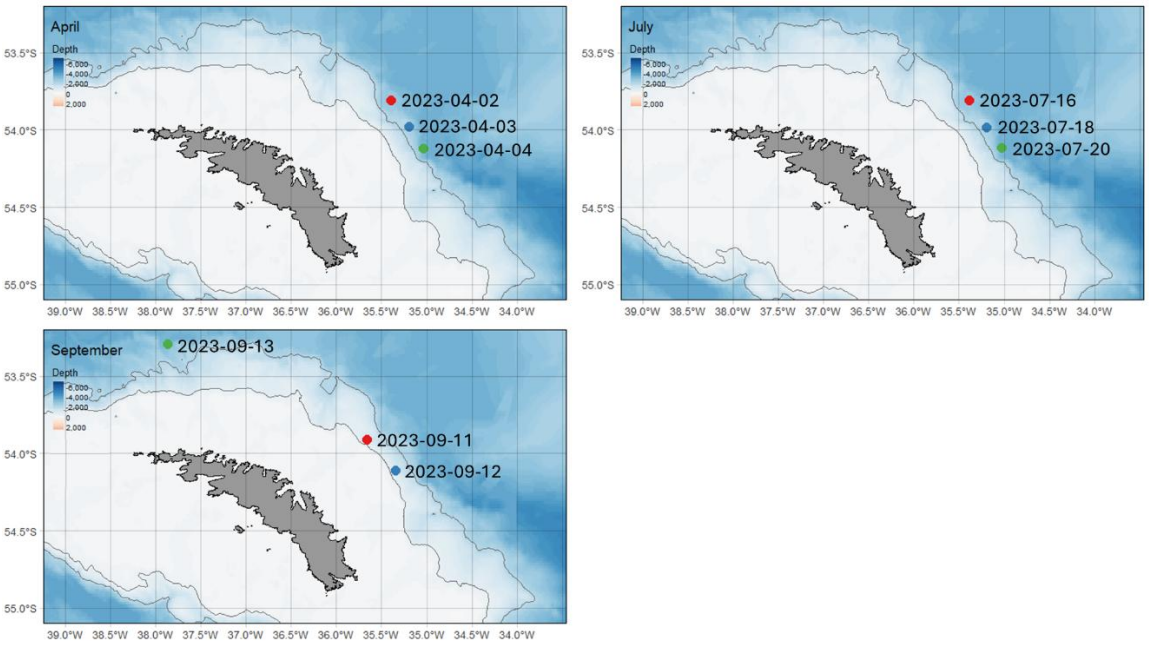

Figure S7. *Locations of CTD deployments in April, July, and September 2023 at South Georgia collected by the British Antarctic Survey. Deployment locations are overlaid onto a map showing the bathymetry around South Georgia, with contour lines representing the 500 and 2000 m isobath.*

Whilst individual CTD temperature profiles were not particularly well replicated by the GLORYSv12 temperature data, when the same data were aggregated to a monthly scale there was much better agreement between the two data sources (**Figure S8**). This was particularly so for April and July, where the major characteristics of the CTD-derived temperatures were well replicated by the GLORYSv12 data (**Figure S8**). However, deployments in September showed a relatively larger difference, even when aggregated across deployments, with the GLORYSv12 data tending to overestimate temperature in the near surface mixed layer, while underestimating temperatures for depths greater than 200m (**Figure S8**).

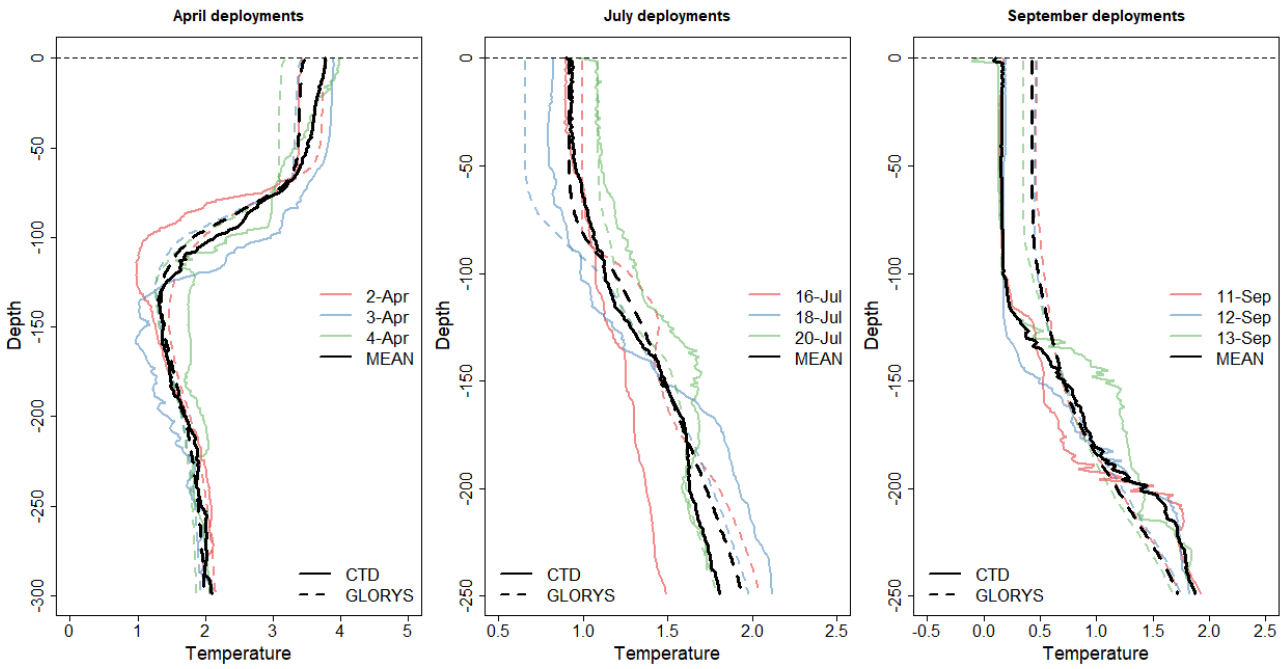

Figure S8. *Vertical temperature profiles derived from CTD deployments, and compared to equivalent data, matched to time and location, extracted from the GLORYSv12 dataset. In addition to individual profiles from each CTD deployment, we also show the aggregate profile for each month by averaging across the available data.*

Section 5: Additional figures

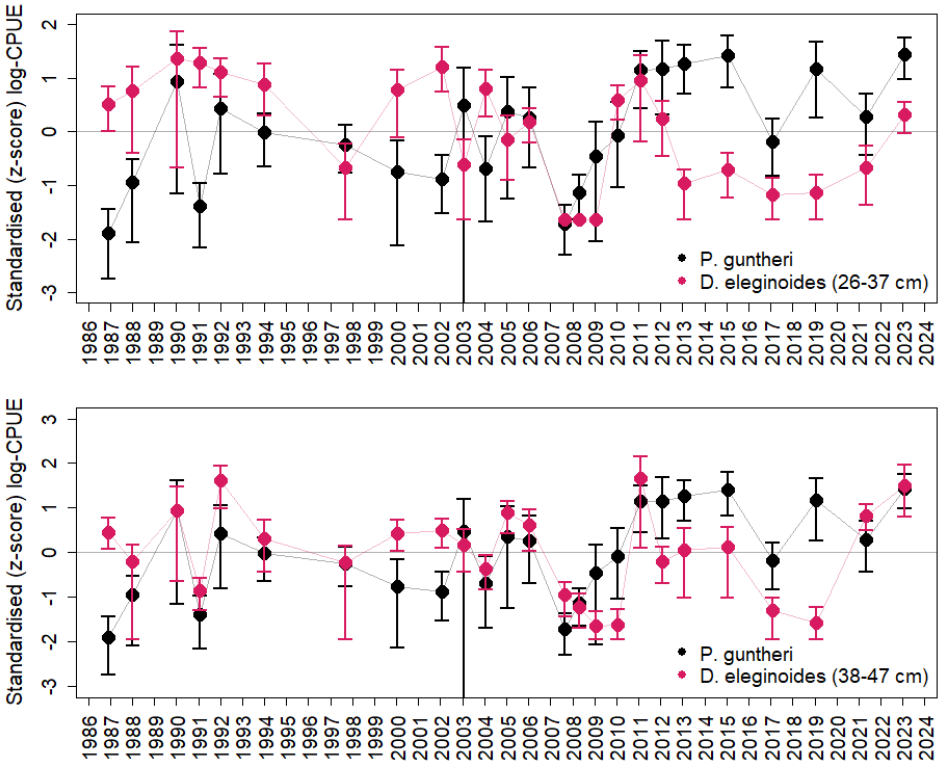

Figure S9. *Comparisons of interannual variability in CPUE at Shag Rocks between Patagonotothen guntheri and 26-37 cm (upper panel) and 38-47 cm (lower panel) size-classes of Patagonian toothfish. Values correspond to standardised (z-score) log-CPUE based on interannual variability, along with bootstrapped 95% confidence intervals.*